Final Project Report for Task 6 of the Option 3 Period
Navy SBIR 2008.2 - Topic N08-131, Contract No. N68335-16-C-0088

Innovative Approaches to Flaw-Tolerant Design and Certification of Airframe Components
Report on NACA Data – Task 6

Ricardo Actis and Barna Szabó

Engineering Software Research and Development, Inc.
111 West Port Plaza, Suite 825
St. Louis, MO 63146

September 26, 2017

Revised: October 16, 2017

DISCLAIMER

This work was sponsored by the Navy SBIR Office under contract No. N68335-16-C-0088. The views and conclusions contained herein are those of the authors and should not be interpreted as necessarily representing the official policies or endorsements, either expressed or implied, of the sponsoring agency or the U.S. Government.

REPORT DOCUMENTATION PAGE

Form Approved
OMB No. 0704-0188

1. REPORT DATE *(DD-MM-YYYY)*	2. REPORT TYPE	3. DATES COVERED *(From - To)*
16-10-2017	Final	Nov. 2015 - Nov. 2017

4. TITLE AND SUBTITLE
Innovative Approaches to Flaw-Tolerant Design and Certification of Airframe Components

Report on NACA Data - Task 6

5a. CONTRACT NUMBER
N68335-16-C-0088

5b. GRANT NUMBER

5c. PROGRAM ELEMENT NUMBER

6. AUTHOR(S)
Ricardo Actis
Barna Szabó

5d. PROJECT NUMBER
SBIR N08-131

5e. TASK NUMBER
6

5f. WORK UNIT NUMBER

7. PERFORMING ORGANIZATION NAME(S) AND ADDRESS(ES)
Engineering Software Research and Development, Inc.
111 West Port Plaza, Suite 825
St. Louis, MO 63146

8. PERFORMING ORGANIZATION REPORT NUMBER
N68335-16-C-0088

9. SPONSORING/MONITORING AGENCY NAME(S) AND ADDRESS(ES)
NAVAIR SBIR Program Office, Code 4.0T
Bldg. 2109, Rm. 122
Naval Air Warfare Center Aircraft Division
48150 Shaw Rd.
Patuxent River, MD 20670-1906

10. SPONSOR/MONITOR'S ACRONYM(S)
NAVAIR SBIR Office

11. SPONSORING/MONITORING AGENCY REPORT NUMBER

12. DISTRIBUTION AVAILABILITY STATEMENT
Approved for public release; distribution unlimited. NAVAIR Public Release Authorization 2017-966.

13. SUPPLEMENTARY NOTES

14. ABSTRACT
This report presents the results of the work performed with unflawed notched NACA specimens used in connection with Contract No. N68335-10-C-0428 – Option 1, Task 1.3. One of the unique aspects of the analytical approach developed in this work is the use of a family of damage accumulation models for ranking in-service damage based on fatigue criticality. The proposed stress-based damage accumulation models, using the integral average of a function of stress over a solution-dependent volume, were tested against available experimental data available in the literature for notched fatigue specimens. This report provides step by step procedures to obtain the reference S-N curve from unnotched specimens of 24S-T3, 75S-T6 and SAE 4130, the calibration procedure to obtain the Beta-HSV curves for each material, and the prediction of fatigue life based on the calibration curve, including the measure of the difference between model prediction and the experimental results.

15. SUBJECT TERMS
Notch Fatigue, Stress Life, Life Prediction, Highly Stressed Volume, High Cycle Fatigue, Model Calibration, NACA

16. SECURITY CLASSIFICATION OF:			17. LIMITATION OF ABSTRACT	18. NUMBER OF PAGES	19a. NAME OF RESPONSIBLE PERSON
a. REPORT	b. ABSTRACT	c. THIS PAGE	SAR	63	David T. Rusk
Unclassified	Unclassified	Unclassified			19b. TELEPONE NUMBER (*Include area code*) 301 342-9428

Table of Contents

List of Figures

List of Acronyms and Symbols

A1, A2, A3	Parameters of the random fatigue limit model
AIC	Akaike information criterion
α	Material-dependent parameter
β	Characterizing parameter of stress-based damage accumulation models
BF	Bayes factor
CBM	Condition-Based Maintenance
CDF	Cumulative Distribution Function
DMP	Data Management Portal
FTD	Flaw Tolerant Design
G_α	Predictors of damage accumulation
γ	Parameter to define the highly-stressed volume
HSV	Highly Stress Volume of material
HSA	Highly Stress Area of material
I_1	First stress invariant
Kt	Stress concentration factor
$L(\theta)$	The likelihood function
$LL(\theta)$	The log likelihood function
N	Number of fatigue cycles
N_f	Number of cycles to failure
NACA	National Advisory Committee for Aeronautics
PFD	Probability Density Function
Pr	Probability density function
R	Load cycle ratio
S_{max}	Maximum test stress
S_{min}	Minimum test stress
σ_a	Stress amplitude
σ_{max}	Maximum normal stress
σ_{min}	Minimum normal stress
σ_{eq}	Equivalent stress
$\overline{\sigma}$	von Mises stress
Z	Z-score

1 Executive Summary

This report presents the results of the work performed with unflawed notched NACA specimens used in connection with Contract No. N68335-10-C-0428 – Option 1, Task 1.3.

The integrated software system and computational framework developed by ESRD under the Navy SBIR 2008.2 Phase II project – Topic N08-131: *Innovative Approaches to Flaw-Tolerant Design and Certification of Airframe Components* is a new technology ideally suited to model and analyze structural damage that exceeds existing repair limits; to rank in-service damage based on fatigue criticality, not just damage size; to enable the quantitative assessment of risks to flight safety from using condition-based maintenance (CBM) to delay or eliminate fleet inspection requirements; to meet CBM need to move flaw-damaged component removals from unscheduled to scheduled maintenance action by enabling prediction of remaining life.

One of the unique aspects of the approach is the development of a family of damage accumulation models for ranking in-service damage based on fatigue criticality. The proposed stress-based damage accumulation models, using the integral average of a function of stress over a solution-dependent volume, were tested against available experimental data available in the literature for notched fatigue specimens and with flaw-seeded fatigue data provided by the US Navy. The characterizing parameter of the models of damage accumulation (β) was correlated with the highly stressed volume (*HSV*) of material around the flaw to allow the generalization of the calibration work performed for flaw seeded specimens to components with flaws of various sizes and shapes.

This report presents the work performed with unflawed notched NACA specimen and provides step by step procedures to obtain the reference S-N curve from unnotched specimens of 24S-T3, 75S-T6 and SAE 4130, the calibration procedure to obtain the β-*HSV* curves for each material, and the prediction of fatigue life based on the calibration curve, including the measure of the difference between model prediction and the experimental results. The report includes all data extracted from the relevant NACA reports, which is available in the SimGov Data Management Portal https://ftd.esrd.com.

Acknowledgments

The authors are grateful to David Rusk, TPOC, for his valuable advice concerning various aspects of the work presented herein.

2 Task 6 – Report on NACA Data

2.1 Task description

The following description corresponds to Task 6 of the Option 3 Period of the contract:

- *Prepare a detailed report of the work performed with unflawed notched NACA specimens used in connection with Contract No. N68335-10-C-0428 – Option 1, Task 1.3. Task will document the step by step procedure to obtain the reference S-N curve from unnotched specimens of 24S-T3, 75S-T6 and SAE 4130, the calibration procedure to obtain the β-HSV curves for each material, and the prediction of fatigue life based on the calibration curve, including the measure of the difference between model prediction and the experimental results. The report shall include all data extracted from the relevant NACA reports available in the SimGov Data Management Portal https://ftd.esrd.com*

2.2 Summary of NACA data

The NACA data consists of a collection of technical notes containing axial-load fatigue test results for unnotched and notched sheet specimens of 24S-T3, 75S-T6 aluminum alloys and SAE 4130 steel, as well as all the tabulated data in spreadsheets deployed in the SimGov Data Management portal (see Appendix 4 for details). The references for the technical notes are as follows:

- Grover HJ, Bishop SM and Jackson LR, *Fatigue Strength of Aircraft Materials. Axial-Load Fatigue Tests on Unnotched Sheet Specimens of 24S-T3 and 75S-T6 Aluminum Alloys and of SAE 4230 Steel*. NACA Technical Note 2324, March 1951.
- Grover HJ, Bishop SM and Jackson LR, *Fatigue Strength of Aircraft Materials. Axial-Load Fatigue Tests on Notched Sheet Specimens of 24S-T3 and 75S-T6 Aluminum Alloys and of SAE 4230 Stainless Steel with Stress Concentrations Factors of 2.0 and 4.0*. NACA Technical Note 2389, June 1951.
- Grover HJ, Bishop SM and Jackson LR, *Fatigue Strength of Aircraft Materials. Axial-Load Fatigue Tests on Notched Sheet Specimens of 24S-T3 and 75S-T6 Aluminum Alloys and of SAE 4230 Stainless Steel with Stress Concentrations Factors of 5.0*. NACA Technical Note 2390, June 1951.
- Grover HJ, Bishop SM and Jackson LR, *Fatigue Strength of Aircraft Materials. Axial-Load Fatigue Tests on Notched Sheet Specimens of 24S-T3 and 75S-T6 Aluminum Alloys and of SAE 4230 Stainless Steel with Stress Concentrations Factors of 1.5*. NACA Technical Note 2639, February 1952.

- Grover HJ, Bishop SM and Jackson LR, *Fatigue Strength of Aircraft Materials. Axial-Load Fatigue Tests on Notched Sheet Specimens of 2024-T3 and 7075-T6 Aluminum Alloys and of SAE 4230 Stainless Steel with notched radii of 0.004 and 0.070 inch*. NASA Technical Note D-111, September 1959.

The material properties and thicknesses of the NACA specimens are shown in Table 1, while the details of the test records are summarized in Table 2 (values in brackets in the last 3 columns are the number of specimens that failed during the fatigue test).

Table 1: Material Properties of NACA specimens

Material	Thickness (in)	Grain Direction	Average Tensile Propoerties			Average Compressive Properties	
			Elongation in 2-in (%)	Yield Strength 0.2% Offset (psi)	Ultimate Strength (psi)	Yield Strength (psi)	Modulus of Elasticity (psi)
24S-T3	0.090	with	18.20	54,000	73,000	44,500	10,650,000
		cross	18.30	50,000	71,000	50,500	10,450,000
75S-T6	0.090	with	11.40	76,000	82,500	74,000	10,450,000
		cross	11.00	75,000	82,500	78,500	10,550,000
SAE 4130	0.075	with	14.25	98,500	117,000	86,000	30,400,000
		cross	12.50	101,000	120,000	97,000	31,300,000

Table 2: Summary of the 928 available fatigue test records

#	Description						Number of specimes (failed)		
	Specimen type	NACA Reference	Notch Radius (in)	Nominal Kt	Actual Kt	HSA (in^2)	24S-T3	75S-T6	SAE 4130
1	Unnotched	TN-2324	12.000	1.00	1.00	Test Section	53 (44)	83 (71)	48 (34)
2	Open hole	TN-2389	1.5000	2.00	2.11	2.898E-02	39 (34)	38 (34)	27 (22)
3	Edge notch		0.3175	2.00	2.17	4.325E-03	42 (38)	39 (33)	41 (35)
4	Fillet notch		0.1736	2.00	2.19	9.561E-04	32 (27)	31 (29)	31 (26)
5	Edge notch		0.0570	4.00	4.43	1.827E-04	34 (29)	32 (27)	39 (34)
6	Fillet notch		0.0195	4.00	4.83	1.618E-05	36 (32)	28 (24)	32 (28)
7	Edge notch	TN-2390	0.0313	5.00	5.83	5.888E-05	46 (40)	47 (41)	42 (38)
8	Edge notch	TN-2369	0.7600	1.50	1.62	2.875E-02	31 (27)	31 (30)	24 (21)
9	Edge notch	TN-D-111	0.0035	4.00	4.48	5.908E-07	17 (13)	17 (14)	16 (13)
10	Edge notch		0.0710	4.00	4.41	3.324E-04	19 (15)	20 (15)	19 (16)

2.3 Reference S-N Curve: Implementation of Random Fatigue Models

Mathematical models devised for the prediction of damage accumulation in high cycle fatigue consist of a problem of linear elasticity plus two sub-models: a predictor $\mathcal{P}$ and a statistical model $\mathcal{S}$. A predictor is a functional of the solution of the problem of linear elasticity (or, more generally, small-strain solid mechanics) intended for the generalization of the results of uniaxial fatigue data, also known as S-N data, to triaxial stress conditions. Details are available in [1].

Statistical models are formulated for the quantification and generalization of the statistical dispersion of S-N data. The information collected from constant cycle fatigue tests consists of (a) the maximum test stress S_{max}, (b) the cycle ratio R, which is defined as the ratio of the minimum test stress S_{min} to the maximum test stress S_{max}, (c) the number of cycles at which failure occurred or the test was stopped N_f , (d) an indication whether the test was stopped prior to failure (runout) and (e) notes indicating unusual events such as buckling, failure at the grips or failure outside of the test section that may have occurred. Typical statistical models used in the analysis of fatigue data and their properties are described in [2]. The implementation of two random fatigue limit models is described in this document. These models are based on the papers of Pascual and Meeker [3], [4]. Additional discussion and analysis are available in [2].

2.3.1 Formulation of statistical model $\mathcal{S}_1$

We define the equivalent stress σ_{eq} as [5]:

$$\sigma_{eq} = S_{\max}\left(\frac{1-R}{2}\right)^{1/2} \qquad \textbf{Eq. 1}$$

It is assumed that $\log_{10} N_f$ is normally distributed:

$$\log_{10} N_f \approx \mathrm{N}(\mu, s) \qquad \textbf{Eq. 2}$$

The mean μ is defined by

$$\mu = A_1 - A_2 \log_{10}(\sigma_{eq} - A_3), \quad 0 \le A_3 < \sigma_{eq} \qquad \textbf{Eq. 3}$$

where A_3 is the fatigue limit. In random fatigue limit models A_3 is a random variable. We assume that $\log_{10} A_3$ is normally distributed:

$$\log_{10} A_3 \approx \mathrm{N}(\mu_f, s_f) \qquad \textbf{Eq. 4}$$

We assume that the standard deviation s is constant. Therefore the statistical model is characterized by five parameters $\theta = \{A_1\ A_2\ s\ \mu_f\ s_f\}$. Another statistical model labeled $\mathcal{S}_2$, which has six parameters, is described in Appendix 1.

We introduce the notation $w = \log_{10} N_f$, $v = \log_{10} A_3$ and invoke two fundamental theorems in statistics; the product rule and marginalization. The product rule applied to the random fatigue limit model is:

$$\Pr(w, v \mid \sigma_{eq}) = \Pr(w \mid \sigma_{eq}, v) \Pr(v \mid \sigma_{eq}) \quad \textbf{Eq. 5}$$

where Pr stands for the probability density function. The equation of marginalization is

$$\Pr(w \mid \sigma_{eq}) = \int_{-\infty}^{\log_{10} \sigma_{eq}} \Pr(w, v \mid \sigma_{eq})\, dv. \quad \textbf{Eq. 6}$$

Therefore the probability of w given σ_{eq} is:

$$\Pr(w \mid \sigma_{eq}) = \int_{-\infty}^{\log_{10} \sigma_{eq}} \Pr(w \mid \sigma_{eq}, v) \Pr(v \mid \sigma_{eq})\, dv. \quad \textbf{Eq. 7}$$

According to Eq. (2) w has normal distribution with mean μ and standard deviation s. Therefore the first term of the integrand in Eq. (7) is the probability density function:

$$F(w, \sigma_{eq}, v) \equiv \Pr(w \mid \sigma_{eq}, v) = \frac{\exp(-(w - \mu(\sigma_{eq}, 10^v))^2 / (2s^2))}{s\sqrt{2\pi}}. \quad \textbf{Eq. 8}$$

The second term of the integrand in Eq. (7) follows from Eq. (4). By hypothesis the probability density of v is:

$$f(v) \equiv \Pr(v \mid \sigma_{eq}) = \frac{\exp(-(v - \mu_f)^2 / 2s_f^2)}{s_f \sqrt{2\pi}}. \quad \textbf{Eq. 9}$$

Therefore the marginal probability density function of w, given σ_{eq}, is:

$$F_M(w, \sigma_{eq}) \equiv \Pr(w \mid \sigma_{eq}) = \int_{-\infty}^{\log_{10} \sigma_{eq}} F(w, 10^v)\, f(v)\, dv. \quad \textbf{Eq. 10}$$

The marginal cumulative distribution function (CDF) of w, given σ_{eq}, is:

$$\Phi_M(w, \sigma_{eq}) = \int_{-\infty}^{w} F_M(t, \sigma_{eq})\, dt = \frac{1}{2} \int_{-\infty}^{\log_{10} \sigma_{eq}} \left(1 + \operatorname{erf}\left(\frac{w - \mu(\sigma_{eq}, 10^v)}{s\sqrt{2}}\right)\right) f(v)\, dv. \quad \textbf{Eq. 11}$$

Given a statistical model characterized by a set of parameters θ, and a set of independent observations $(w_i, \sigma_{eq}^{(i)})$, $(i = 1, 2, \ldots, m)$ the likelihood function is

$$L(\theta) = \prod_{i=1}^{m} \left[F_M(w_i, \sigma_{eq}^{(i)})\right]^{1-\delta_i} \left[1 - \Phi_M(w_i, \sigma_{eq}^{(i)})\right]^{\delta_i} \quad \textbf{Eq. 12}$$

where

$$\delta_i = \begin{cases} 0 & \text{if the test resulted in failure} \\ 1 & \text{if the test was stopped before failure} \end{cases} \qquad \textbf{Eq. 13}$$

The maximum likelihood estimate of θ, denoted by $\hat{\theta}$, maximizes $L(\theta)$, or equivalently, the log likelihood function $LL(\theta)$ defined by

$$LL(\theta) = \sum_{i=1}^{m} (1-\delta_i) \ln\left(F_M(w_i, \sigma_{eq}^{(i)})\right) + \sum_{i=1}^{m} \delta_i \ln\left(1 - \Phi_M(w_i, \sigma_{eq}^{(i)})\right). \qquad \textbf{Eq. 14}$$

2.3.2 Theoretical design curves

The theoretical design curve $d_k(\sigma_{eq})$ is the set of points $(\log_{10} N, \sigma_{eq})$ that satisfy the condition

$$\text{Prob}(N_f \le N \mid \sigma_{eq}, \hat{\theta}_k) = p \qquad \textbf{Eq. 15}$$

where k identifies the statistical model and p represents the acceptable probability of failure which is typically a small number, such as $p = 10^{-5}$. Theoretical design curves are obtained through application of statistical models well beyond their range of calibration. Furthermore, theoretical design curves strongly depend on the choice of the statistical model. Therefore considerable aleatory and epistemic uncertainties exist. Because events of such low probability occur very rarely, validation of statistical models with respect to design curves is not feasible.

The setting of factors of safety, which are to account for aleatory and epistemic uncertainties, is burdened by the same uncertainties. Therefore subjective judgment in setting factors of safety cannot be avoided. For further discussion we refer to [6].

2.3.3 Implementation of the statistical model

The implementation is based on Matlab R2016a (9.0.0.341360) 64 bit (win64). The main routine for Statistical Model $\mathcal{S}_1$ is a Matlab function called MMPDSmodel1RFL(mat).m. The argument refers to the material type; mat = 1, 2, 3 corresponds to 24S-T3, 75S-T6 aluminum alloys and SAE 4130 steel respectively. This function performs the following operations:

1. Reads the material data identified by the argument mat. The data are in the file NACA Unnotched Specimen 4-13-16.xlsx.
2. Calls the Matlab function *mle* (maximum likelihood estimate) which returns parameters for user-specified statistical models. It accounts for censored data (runouts). The PDF and the CFD functions are called *custpdfRFL1.m* and *custcdfRFL1.m* respectively.

The integrals in equations (10) and (11) have to be evaluated numerically. In the test implementation the Matlab function *integral* is used for this purpose with tolerance settings $'\text{AbsTol}' = 10^{-12}$, $'\text{RelTol}' = 10^{-12}$.

The maximum likelihood estimate involves the solution of a highly nonlinear problem for the parameters of the statistical model. Typically there are multiple local maxima. The maximum is sought in the neighborhood of user-provided seed values of the parameters. One can never be certain that the global maximum of $LL(\theta)$, denoted by $LL(\hat{\theta})$, was found. It is advisable therefore to try several seed values and select the set of parameters that corresponds to the maximum value of the log likelihood function given by Eq. (14). Estimation of seed values is discussed separately.

3. Computes the log likelihood function $LL(\hat{\theta})$ and the Akaike information criterion (AIC).

4. Plots the S-N data and the function μ defined by Eq. (3). It also plots the theoretical design curve at probability level $p = pr$. For the definition of p see Eq. (15). The design curve parameters A_1, A_2, A_3 are returned in vector b. The pertinent commands are as follows:

```
% Design curve at probability pr
pr = 0.001;
[NAx,SA,G] = DesignCurve1RFL(mat);
Fnorm2 = contour(NAx,SA,G,[pr pr],'r');
b = DesignCurveFit1(Fnorm2);
```

An example is shown in Figure 1.

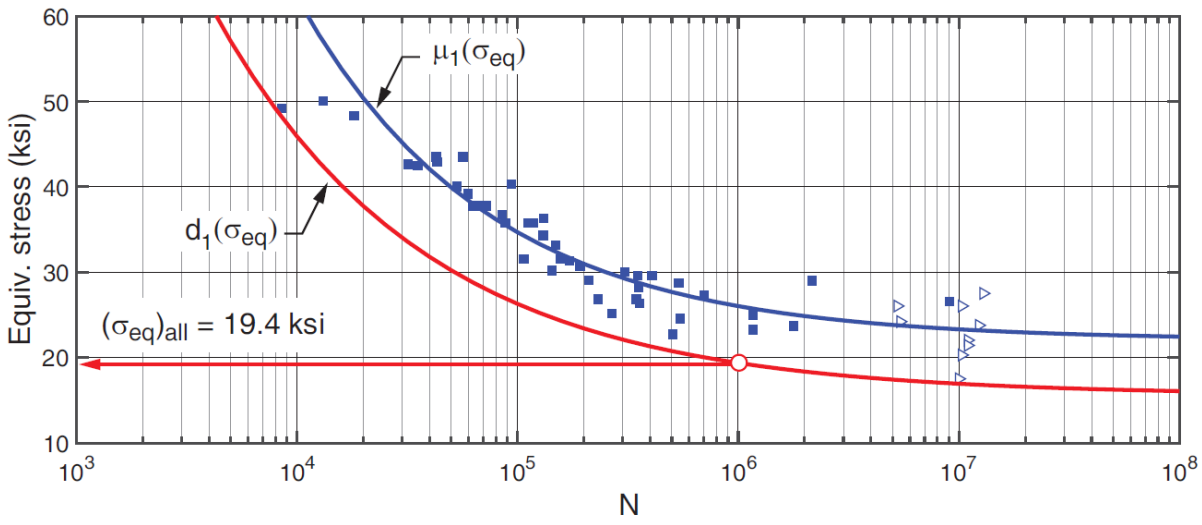

Figure 1: S-N data for 24S-T3 aluminum alloy. The mean corresponding to Model $\mathcal{S}_1$ is labeled $\mu_1(\sigma_{eq})$, the theoretical design curve corresponding to $p = 0.001$ is labeled $d_1(\sigma_{eq})$. Runouts are represented by the open triangular markers.

Theoretical allowable value

Given a theoretical design curve and the number of design cycles N, it is possible to compute the theoretical allowable value from

$$\left(\sigma_{eq}\right)_{all} = d_1^{-1}(N) \qquad \textbf{Eq. 16}$$

For example, referring to Figure 1, for $N = 10^6$ we have $(\sigma_{eq})_{all}$ = 19.4 ksi.

Tolerance settings

The computations were performed with the following tolerance settings:

```
Display: 'off'
MaxFunEvals: 1000000
MaxIter: 1000000
TolBnd: 1.0000e-06
TolFun: 1.0000e-06
TolX: 1.0000e-06
GradObj: 'on'
DerivStep: 1
FunValCheck: 'on'
```

Seed parameters

The maximum likelihood estimate requires seed parameters which are used by the Matlab function *mle* as the starting parameter values in the iterative process for estimating $\hat{\theta}$.

The user provides an upper and lower bound for A_3, denoted by U and L respectively. These are the bounds of the S-N data in the high cycle range. The interval $U - L$ is divided into m sub-intervals (for example, m = 100).

Letting

$$A_3^{(i)} = L + (i-1)(U-L)/m, \quad i = 1, 2, \ldots, m+1 \qquad \textbf{Eq. 17}$$

we find $A_1^{(i)}$ and $A_2^{(i)}$ by linear regression to fit the data to

$$\log_{10} N_j = A_1^{(i)} - A_2^{(i)} \log_{10}(\sigma_{eq} - A_3^{(i)}) \qquad \textbf{Eq. 18}$$

where j identifies all data points $\left(\sigma_{eq}^{(j)}, N_j\right)$ that satisfy the criterion

$$\sigma_{eq}^{(j)} - A_3^{(i)} > 0. \qquad \textbf{Eq. 19}$$

Runouts are treated in the same way as other points. We denote the number of data points by n_i, compute the variance of each i,

$$V_i = \frac{1}{n_i}\sum_{j=1}^{n_i}\left(\sigma_{eq}^{(j)} - \left(A_3^{(i)} + 10^{-\left(\log_{10} N_j - A_1^{(i)}\right)/A_2^{(i)}}\right)\right)^2 \qquad \textbf{Eq. 20}$$

and identify the index *i* that corresponds to the smallest variance. We denote that value by *I*. To estimate the seed value corresponding to the standard deviation for model $\mathcal{S}_1$, we compute the sample standard deviation:

$$S = \left(\frac{1}{n_I} \sum_{j=1}^{n_I} \left(\log_{10} N_j - \left(A_1^{(I)} - A_2^{(I)} \log_{10} (\sigma_{eq}^{(j)} - A_3^{(I)}) \right) \right)^2 \right)^{1/2} \quad \textbf{Eq. 21}$$

The computations are performed using the Matlab function *SeedValuesLS1.m*. The seed values for Model $\mathcal{S}_1$ are:

$$\theta_{seed}^{(1)} = \left\{ A_1^{(I)} \; A_2^{(I)} \; S \log_{10} \left(A_3^{(I)} \right) \; 0.05 \right\} \quad \textbf{Eq. 22}$$

where the number 0.05, the seed value for s_f , was determined by trial and error.

Note: All the matlab functions and input data for both statistical models are contained in the files: Model S1 Archived.zip and Model S2 Archived.zip (see Appendix 4 for details).

2.3.4 Computed model parameters

The computed statistical parameters, the parameters that define the theoretical design curve, the input parameters *L*, *U*, s_f and the corresponding output parameters consisting of the log likelihood estimate $LL(\hat{\theta})$ and the Akaike information criterion (AIC) are displayed in Figure 2.

NACA materials: Statitical Model S1			
	24S-T3	75S-T6	SAE 4130
A1	7.193	6.336	7.228
A2	1.992	1.531	1.764
A3	22.06	26.79	54.09
s	0.125	0.115	0.249
s_f	0.0488	0.0432	0.0389

Parameters for the design curves P=1/1000			
	24S-T3	75S-T6	SAE 4130
A1	7.271	6.411	7.581
A2	2.210	1.737	2.318
A3	15.615	19.694	40.602

Seed and output parameters			
	24S-T3	75S-T6	SAE 4130
U	35	35	75
L	15	15	45
s_f	0.05	0.05	0.05
LL	-576.73	-881.37	-477.71
AIC	1163.5	1772.7	965.4

Parameters for the design curves P=1/100000			
	24S-T3	75S-T6	SAE 4130
A1	7.252	6.393	7.621
A2	2.271	1.796	2.480
A3	13.767	17.629	36.520

Figure 2: Unnotched NACA data. Computed and input parameters for statistical model 1.

The parameters of the theoretical design curve are computed by the function *DesignCurveMainRFL(mat,p)* where *mat* identifies the material and *p* is the probability in Eq. (15). The AIC is a measure of the goodness of fit between the statistical model and the data. The data corresponding to AIC was computed using the method used in [2] which differs by scaling from the method used in [4].

The goal is to minimize this value, given the data. Since the statistical model depends on the values of the seed parameters, the seed parameters that lead to the lowest AIC value should be used. The statistical parameters that maximize the log likelihood function given by Eq. (14) minimize AIC.

2.3.4.1 Reference S-N curve for aluminum 24S-T3

The fatigue data of 93 unnotched specimen extracted from NACA-TN-2324, Table 2 is tabulated in the Excel file: naca-tn-24S-T3-(Raw Data).xlsx, worksheet "Kt=1 data". Of the 93 specimens, 10 were runouts and 11 were disqualified tests[1]. Fifty three (53) data points were used for determining the S-N curve of the material (29 specimens tested with $S_{max} > 1.06\ S_Y$, where S_{max} is the maximum test stress in the load cycle and S_Y is the average tensile yield strength of the material in the grain direction shown in Table 1, were excluded). The median S-N curve of the material and the two theoretical design curves based on the parameters of the statistical model $\mathcal{S}_1$ are shown in Figure 3.

	24S-T3
A1	7.193
A2	1.992
A3	22.06
s	0.125
s_f	0.0488

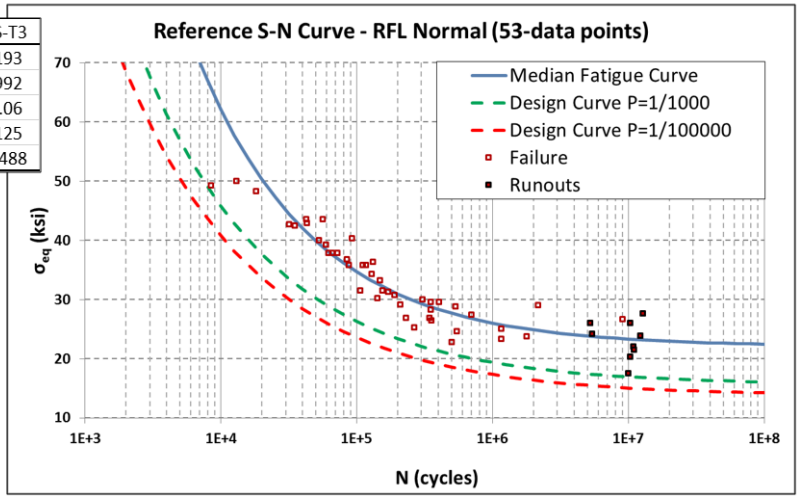

Figure 3: Median S-N curve for aluminum 24S-T3 using the parameters from statistical model 1.

2.3.4.2 Reference S-N curve for aluminum 75S-T6

[1] Most disqualified tests had failures that occurred outside the critical section (the area ½-in at either side of the line of minimum cross-section). A smaller number of failures occurred inside the grips or in a defect (flaw or pit).

The fatigue data of 86 unnotched specimen extracted from NACA-TN-2324, Table 3 is tabulated in the Excel file: naca-tn-75S-T6-(Raw Data).xlsx, worksheet "Kt=1 data". Of the 86 specimens, 12 were runouts and 3 were disqualified tests. Eighty three (83) data points were used for determining the S-N curve of the material (no specimens were tested with $S_{max} > 1.06\ S_Y$).

The median S-N curve of the material and the two theoretical design curves based on the parameters of the statistical model $\mathcal{S}_1$ are shown in Figure 4.

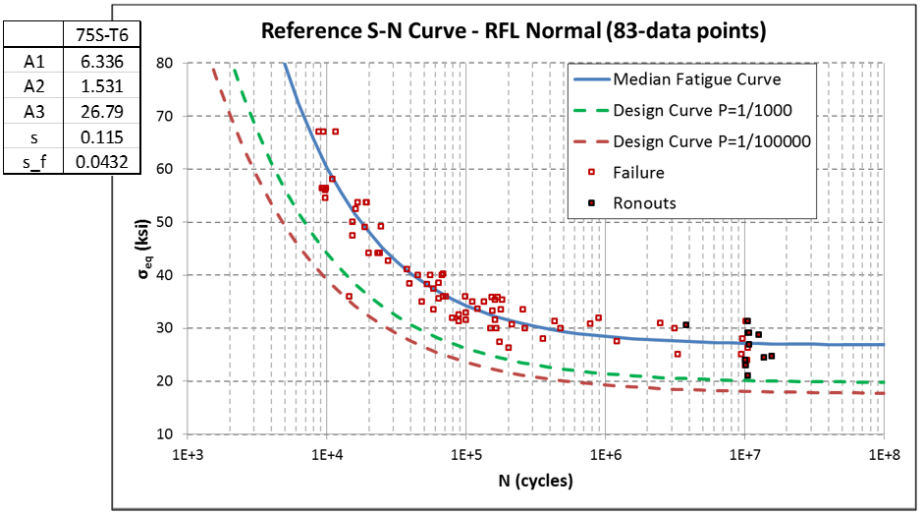

Figure 4: Median S-N curve for aluminum 75S-T6 using the parameters from statistical model 1.

2.3.4.3 Reference S-N curve for SAE 4130 steel

The fatigue data of 59 unnotched specimen extracted from NACA-TN-2324, Table 4 is tabulated in the Excel file: naca-tn-SAE-4130-(Raw Data).xlsx, worksheet "Kt=1 data". Of the 59 specimens, 16 were runouts and 6 were disqualified tests. Forty Eight (48) data points were used for determining the S-N curve of the material (5 specimens tested with $S_{max} > 1.06\ S_Y$, where S_{max} is the maximum test stress in the load cycle and S_Y is the average tensile yield strength of the material in the grain direction shown in Table 1, were excluded). The median S-N curve of the material and the two theoretical design curves (P-quantiles) based on the parameters of the statistical model $\mathcal{S}_1$ are shown in Figure 5.

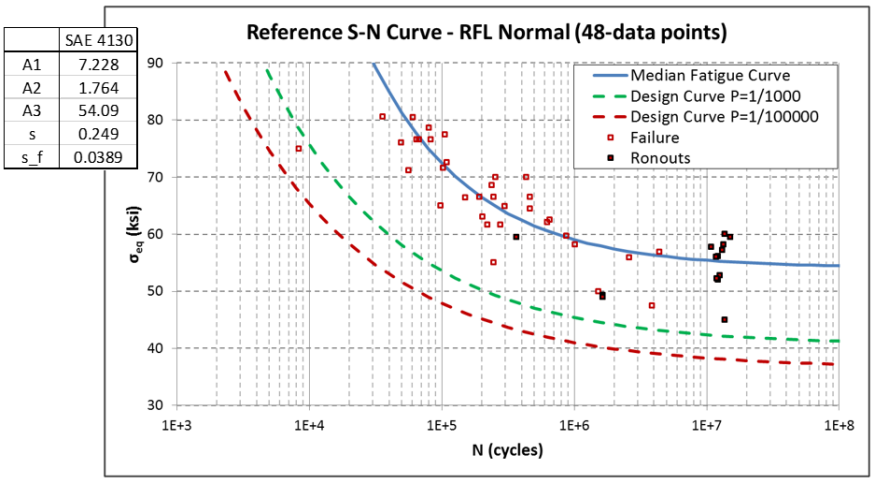

Figure 5: Median S-N curve for SAE-4130 steel using the parameters from statistical model 1.

2.4 Generalization for Notches – Calibration of Predictors

Predictors of damage accumulation are phenomenological models constructed for the purpose of generalizing sets of experimental data obtained in fatigue tests of mechanical or structural components subjected to cyclic loading. Predictors are scalars that depend on the solution of a problem of elasticity, or more generally, a problem of continuum mechanics.

The predictors used in classical high cycle fatigue life estimation depend on the maximum normal stress σ_{max} and the stress amplitude σ_a defined by

$$\sigma_a = \frac{\sigma_{\max} - \sigma_{\min}}{2} = \sigma_{\max}\frac{1-R}{2} \qquad \textbf{Eq. 23}$$

where R, called the cycle ratio, is the ratio of the minimum principal stress σ_{min} to the maximum principal stress at the location of the maximum principal stress. When the linear theory of elasticity is applicable then it is also the ratio of the minimum applied load to the maximum applied load. A family of predictors commonly used in engineering practice for uniaxial stress is:

$$F = \sigma_{eq} = \sigma_{\max}^{1-q}\sigma_a^q, \quad 0 < q < 1 \qquad \textbf{Eq. 24}$$

Where σ_{eq} is called the equivalent stress. Using Eq. (23):

$$F = \sigma_{eq} = \sigma_{\max}\left(\frac{1-R}{2}\right)^q, \quad 0 < q < 1 \qquad \textbf{Eq. 25}$$

The special case of q = 1/2 is one of the predictors proposed by Smith, Watson and Topper in [5] and used in this work for determining the S-N curve of the materials.

Predictors are formulated with the objective to generalize results of fatigue tests performed on coupons subjected to constant or smoothly varying uniaxial or, less frequently, biaxial stress conditions to arbitrary tri-axial stress conditions.

Specifically, we investigated the performance of a family of predictors defined as follows:

$$F = G_\alpha = \frac{1}{V_c}\int_{\Omega_c}\left(\alpha I_1 + (1-\alpha)\bar{\sigma}\right)dV\left(\frac{1-R}{2}\right)^{1/2}, \quad 0 \le \alpha \le 1 \qquad \textbf{Eq. 26}$$

where I_1 is the first stress invariant, $\bar{\sigma}$ is the von Mises stress, α is a material-dependent parameter determined by calibration and V_c is the volume of the domain of integration defined by

$$\Omega_c = \left\{\vec{x} \mid \sigma_1 \ge \beta\,\sigma_{peak}\right\} \qquad \textbf{Eq. 27}$$

Where $\vec{x}$ is the position vector, σ_1 is the first principal stress, $0 < \sigma_{peak}$, is the maximum stress at the stress raiser, β is an experimentally-determined variable that depends on the material, the definition of G_α and the geometric features of the stress raiser.

The effect of the geometric features of the stress raisers is quantified by the highly stressed volume *HSV* which is defined by:

$$HSV = \int_{\Omega_\rho} y(\vec{x})dV \quad \text{where} \quad y = \begin{cases} 1 & \text{when } \sigma_1(\vec{x}) > \gamma\,\sigma_{peak} \\ 0 & \text{otherwise} \end{cases} \qquad \textbf{Eq. 28}$$

The domain of integration Ω_ρ is the neighborhood of a stress raiser. Denoting the position vector of the stress raiser by $\vec{x}_0$ we have $\Omega_\rho = \left\{\vec{x} \mid |\vec{x} - \vec{x}_0| < \rho\right\}$ where ρ is chosen large enough to include all points such that $\sigma_1(\vec{x}) > \gamma\sigma_{peak}$ and small enough to include only one stress raiser or one group of closely spaced stress raisers.

The parameter γ is independent of material properties. Its role is to define the highly stressed volume *HSV* which depends on the stress field in the neighborhood of stress raisers. In a separate investigation it was established that the predicted number of fatigue cycles is not sensitive to the choice of γ and $\gamma = 0.85$ is a reasonable choice. The same value was used in [1]. Henceforth we will also use $\gamma = 0.85$ in this report.

An example of the highly stressed volume for a circular cutout using $\gamma = 0.85$ is shown in Figure 6.

Figure 6: Example of the stress distribution around a circular cutout in a test specimen (left) and the corresponding size of the *HSV* computed using Eq. (28) with $\gamma = 0.85$ (right).

In the special case of uniaxial stress G_α is the equivalent uniaxial stress. The integrand is the generalization of uniaxial stress to triaxial stress conditions considered in this work. Equations (26) to (28) define the functional form of the predictor. The parameters α and β are material-dependent and thus have to be estimated through calibration.

Remark: To the authors' knowledge, using a linear combination of the first stress invariant and the octahedral shear stress for the prediction of fatigue life under tri-axial loading conditions was first proposed by Sines in [8]. There are important differences between the predictor described by Sines and the predictor proposed herein: (a) Sines' predictor is a pointwise quantity whereas the predictor described herein is an integral average over a solution-dependent domain. (b) Sines assumed that I_1 is determined by the static stress and the octahedral shear stress is determined by the alternating stress. No such assumption is made here: Interaction between the mean and alternating stresses is taken into account through the equivalent stress σ_{eq}.

2.4.1 Calibration of the predictor

The calibration of predictors is based on the test records shown in Table 2. In the column labeled **Actual Kt**, the actual stress concentration factors determined from finite element analysis, defined as the ratio of maximum (peak) stress to the average stress in the test section, are shown. In the column labeled **HSA** the highly stressed area is shown. This area, multiplied by the thickness, approximates the highly stressed volume defined in Eq. (28) for $\gamma = 0.85$. In the last 3 columns the specimen count for each material is listed with and without runouts. The number of specimens without counting runouts is in brackets. This count does not include specimens that were tested at stress levels higher than 1.06 S_Y and specimens that were disregarded by the investigators because of flaws, buckling, or failure in the grips as explained in Section 2.3.4. The test records included in the count are called qualified test records.

Each specimen type is identified by the first column entry in Table 2. For each specimen there are a set of m_k qualified test records; ($S_{test}^{(i)}$, N_i, R_i), i = 1, 2, . . . , m_k where $S^{(i)}$ test is the average stress in the gauge section which is defined as the minimum width times the thickness. All the specimen types and the corresponding finite element mesh for each are shown in Appendix 3.

The highly stressed volume *HSV* depends on the geometry and is independent of the magnitude of loading. Therefore the *HSV* has to be computed for each specimen type only once. In planar problems, when the thickness to notch radius ratio is small, the highly stressed area *HSA* multiplied by the thickness is a very close approximation to *HSV*. Some of the specimen types considered in this investigation do not meet this criterion. However a separate investigation showed that the difference between the highly stressed volume and the highly stressed area multiplied by the thickness is negligibly small.

The workflow for determining the value of β for a given value of α is shown schematically in Figure 7. In the calibration process we fix $0 \leq \alpha \leq 1$ at an arbitrary value and estimate β_i by iteration as follows.

- For a given specimen type ① we find by experiment the number of cycles N_i at which the *i*th notched specimen fails ②.
- If the assumption that $G_\alpha(\beta)$ is a proper generalization of σ_{eq} is correct, then the probability distribution of $G_\alpha^{(i)}(\beta_i)$ is the same as that of σ_{eq} and its expected value is $\mu^{-1}(\log_{10} N_i)$ ③ where μ is the calibrated mean defined in Eq. (3).
- We find the value of S_{max} from Eq. (1) ④ and the corresponding value of β_i by iteration ⑤ such that

$$G_\alpha^{(i)}(\beta_i) - \mu^{-1}(\log_{10} N_i) = 0 \quad i = 1, 2, \ldots, m_k \qquad \textbf{Eq. 29}$$

- This results in a sequence of β values ⑥ that depend on (a) the statistical model, (b) the qualified calibration records, (c) the parameter α and (d) the stress field in the neighborhood of the stress raiser of a specimen type, characterized by the highly stressed area *HSA*.

For example, for α = 0.6 and the test record highlighted in Figure 7, the value of σ_{eq} is 35.02 ksi and for R = -1 the corresponding S_{max} has the same value (see Eq. (1)). It was found by iteration that for β = 0.664, $\widetilde{S}_{max} = 34.99$ ksi which differs from the target value of 35.02 by less than 0.1%. This example is shown in Figure 8 for specimen type 2 of 75S-T6, which also shows the variation of β with α for the highlighted test case.

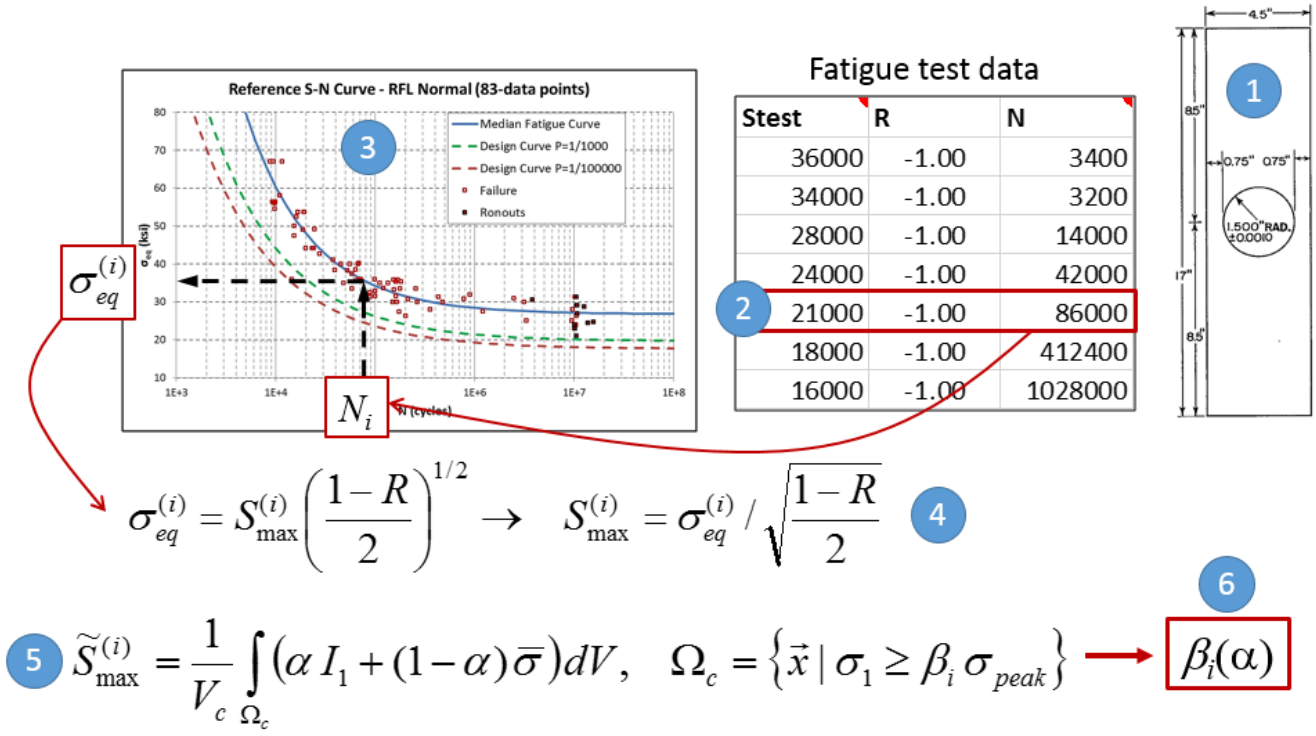

Figure 7: Workflow for the calibration of the predictor.

Stest (psi)	R	N	σ_{eq} (ksi)	S_{max} (ksi)	β	$\tilde{S}_{max}$ (ksi)
28,000	-1.00	14,000	53.73	53.73	0.848	53.74
24,000	-1.00	42,000	39.93	39.93	0.662	39.92
21,000	-1.00	86,000	35.02	35.02	0.664	34.99
18,000	-1.00	412,400	29.75	29.75	0.656	29.77
16,000	-1.00	1,028,000	28.42	28.42	0.740	28.41

α	β
0.0	0.699
0.2	0.688
0.4	0.678
0.5	0.672
0.6	0.664
0.8	0.652
1.0	0.641

Figure 8: Example of calculation of β for $\alpha = 0.6$ for several test results of specimen type 2 (left) and the variation of β with α for the highlighted test result (right).

The value of β for all eight specimen types, all test cases, and for all three materials are available for seven values of α in the Excel files: BetaSummary24S-T3.xlsx, BetaSummary75S-T6.xlsx, BetaSummarySAE-4130.xlsx (see Appendix 4 for details).

The calibration of the predictor involves the following steps:

1. Compute β values corresponding to a sequence $0 \leq \alpha_1, \alpha_2, \ldots, \alpha_n \leq 1$ for each specimen available for calibration. Eight test records identified by line items 2 to 8 and 10 in Table 2 were used for calibration of β as a function of the *HSA*. Two types of fit were used for this relationship:

a. Using linear regression to compute an estimate of the mean values of β, denoted by $\overline{\beta}$, for each α in the form:

$$\overline{\beta}(\alpha_j, HSA) = \mu_\beta = a_j + b_j \log_{10} HSA, \quad j = 1, 2, \ldots, n. \qquad \textbf{Eq. 30}$$

This fitting assumes that for a fixed *HSA*, $\log_{10} \beta$ is normally distributed with standard deviation s_β. The three parameters of the statistical model (a, b, s_β) were estimated by the maximum likelihood method.

b. Logarithm fitting of the arithmetic average of β, denoted by β_{AVG}, for each α in the form:

$$\beta_{AVG}(\alpha_j, HSA) = a_j + b_j \ln HSA, \quad j = 1, 2, \ldots, n. \qquad \textbf{Eq. 31}$$

The parameters of the logarithmic fit and the coefficient of determination were obtained using the Trend line Option in Excel.

An example of the relation β – *HSA* for Aluminum 24S-T3 (α = 0.2) is shown in Figure 9. The value of the arithmetic average of β for the 8 test records characterized by the *HSA* is shown next to the diamond symbol labeled "beta_avg" in the graph; the logarithmic fit is shown with a red solid line characterized by R^2 = 0.933 and labeled "Log(beta_avg)"; while the mean value of β by linear regression is indicated with the green dotted curve labeled as "beta_mean logN".

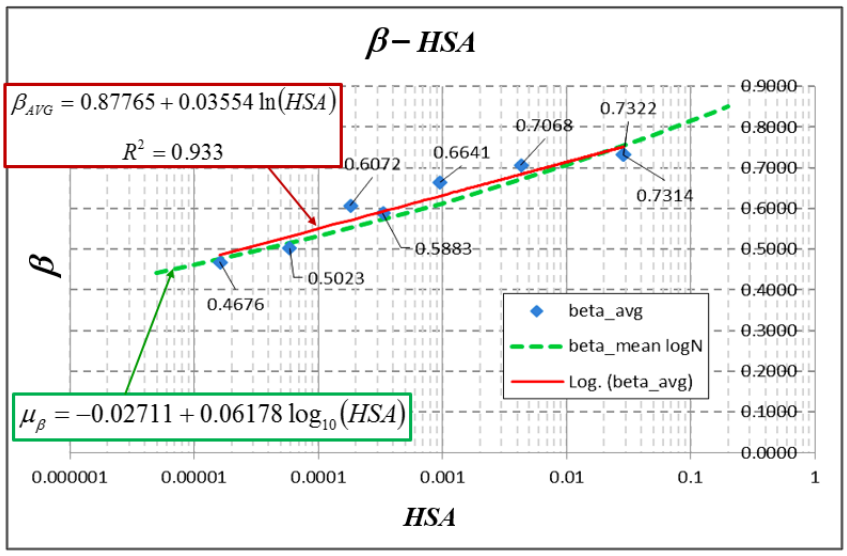

Figure 9: Example of the relation between β and the highly stress area *HSA* for 24S-T3 (α = 0.2).

The parameters of the two types of fitting indicated above are presented in Figure 10 to Figure 12 for aluminum alloys 24S-T3 and 75S-T6 and for steel SAE 4130, respectively, for seven values of α. The data is also available in the Excel file: FittedBetaSummary.xlsx and in the macro Excel files used for the computations: Prediction (24S-T3 SWT)-RFL-Model-1-Alpha-*xx*.xlsm; Prediction (75S-T6 SWT)-RFL-Model-1-Alpha-*xx*.xlsm; Prediction-SAE-4130-RFL-Model-1-Alpha-*xx*.xlsm; with *xx* = 00, 02, 04, 05, 06, 08, 10 (see Appendix 4 for details).

j	α_j	24S-T3					
		$\log_{10}\beta$ is normally distributed			Logarithmic Fit		
		a_j	b_j	Std. Dev	a_j	b_j	R^2
1	0.0	-0.02547	0.05746	0.07773	0.88725	0.03410	0.927
2	0.2	-0.02711	0.06178	0.08202	0.87765	0.03554	0.933
3	0.4	-0.03030	0.06594	0.08625	0.86540	0.03673	0.932
4	0.5	-0.03259	0.06794	0.08823	0.85828	0.03724	0.929
5	0.6	-0.03503	0.06996	0.09026	0.85085	0.03772	0.924
6	0.8	-0.04184	0.07355	0.09375	0.83343	0.03836	0.907
7	1.0	-0.05013	0.07688	0.09676	0.81399	0.03874	0.881

Figure 10: Linear regression and logarithmic fitting parameters for 7 values of α – Aluminum 24S-T3

j	α_j	75S-T6					
		$\log_{10}\beta$ is normally distributed			Logarithmic Fit		
		a_j	b_j	Std. Dev	a_j	b_j	R^2
1	0.0	0.00050	0.05275	0.06330	0.94656	0.03440	0.920
2	0.2	0.00001	0.05675	0.06706	0.93919	0.03598	0.936
3	0.4	-0.00112	0.06101	0.07089	0.93029	0.03755	0.951
4	0.5	-0.00241	0.06307	0.07267	0.92463	0.03825	0.957
5	0.6	-0.00398	0.06522	0.07462	0.91822	0.03892	0.961
6	0.8	-0.00838	0.06942	0.07815	0.90360	0.04012	0.963
7	1.0	-0.01525	0.07331	0.08140	0.88531	0.04099	0.952

Figure 11: Linear regression and logarithmic fitting parameters for 7 values of α – Aluminum 75S-T6

j	α_j	SAE 4130					
		$\log_{10}\beta$ is normally distributed			Logarithmic Fit		
		a_j	b_j	Std. Dev	a_j	b_j	R^2
1	0.0	0.01361	0.07680	0.07121	0.92595	0.04304	0.892
2	0.2	0.01272	0.08172	0.07497	0.91575	0.04440	0.900
3	0.4	0.00994	0.08636	0.07876	0.90278	0.04546	0.906
4	0.5	0.00760	0.08846	0.08071	0.89500	0.04581	0.907
5	0.6	0.00498	0.09055	0.08253	0.88677	0.04613	0.907
6	0.8	-0.00228	0.09420	0.08603	0.86775	0.04642	0.905
7	1.0	-0.01205	0.09701	0.08886	0.84627	0.04630	0.897

Figure 12: Linear regression and logarithmic fitting parameters for 7 values of α – Steel SAE 4130

2. Specimen #9 (Figure 13) is suitable for the selection of the optimal value of α because the highly stressed area (HSA =5.908×10^{-7} in^2) associated with the small notch radius (R = 0.0035 in) is outside the range of the calibration specimens (see Table 2). In the calibration process we fixed α and selected β_i such that $G_\alpha^{(i)}$ lies on the S-N curve, see Figure 7. Consequently any value of $\bar{\beta}$ or β_{AVG} in the range of calibration is an interpolation based on the assumption that the functional form of G_α is correct for any α. The following procedure was used to select the optimal value for α:

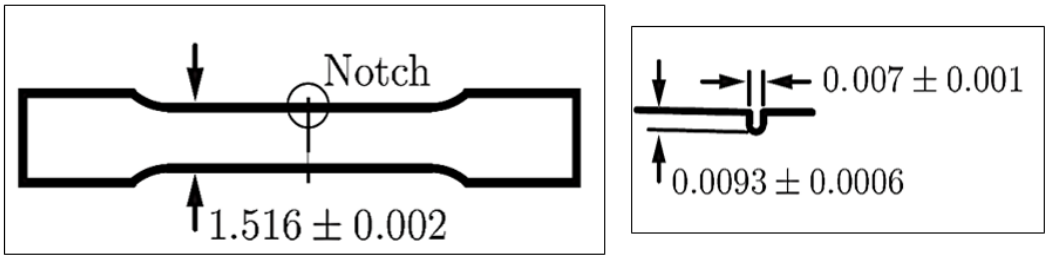

Figure 13: Specimen #9 – Notch detail.

a. Using Eq. 30, compute an estimate of the mean value of $\bar{\beta}(\alpha_j, HSA),\ j = 1, 2, \ldots, n$ for the test records available for the calibration of the predictor.

b. Repeat step (a) using Eq. 31 to compute an estimate of the arithmetic average of $\beta_{AVG}(\alpha_j, HSA),\ j = 1, 2, \ldots, n$ for the test records available for the calibration of the predictor.

The computed values of $\bar{\beta}$ (column heading $(\beta)_{\mathbf{logN}}$) and β_{AVG} (column heading $(\beta)_{\mathbf{AVG}}$) for specimen #9, for 7 values of α, and for all three materials are shown in Table 3.

Table 3: Computed values of $\bar{\beta}$ (Eq. 30) and β_{AVG} (Eq. 31) for specimen #9

j	α_j	Predicted β for Specimen #9					
		24S-T3		75S-T6		SAE 4130	
		$(\beta)_{\mathbf{logN}}$	$(\beta)_{\mathbf{AVG}}$	$(\beta)_{\mathbf{logN}}$	$(\beta)_{\mathbf{AVG}}$	$(\beta)_{\mathbf{logN}}$	$(\beta)_{\mathbf{AVG}}$
1	0.0	0.4136	0.3982	0.4698	0.4532	0.3430	0.3087
2	0.2	0.3873	0.3680	0.4431	0.4232	0.3189	0.2790
3	0.4	0.3622	0.3386	0.4158	0.3918	0.2965	0.2508
4	0.5	0.3501	0.3242	0.4025	0.3760	0.2862	0.2380
5	0.6	0.3382	0.3100	0.3889	0.3601	0.2761	0.2252
6	0.8	0.3163	0.2833	0.3624	0.3282	0.2576	0.2020
7	1.0	0.2958	0.2584	0.3374	0.2975	0.2419	0.1823

c. Using Eq. (26) compute $G_{\alpha_j}^{(i)}$, given $\bar{\beta}(\alpha_j, HSA)$ and $\beta_{AVG}(\alpha_j, HSA)$, for each of the test records corresponding to specimen #9 and for each material. The index *i* refers to a test record. The results are included in the Excel files: RankingData-24S-T3-Specimen-9.xlsx, RankingData-75S-T6-Specimen-9.xlsx, and RankingData-SAE-4130-Specimen-9.xlsx, (see Appendix 4 for details).

d. Using Eq. (14) compute the log likelihood function LL_j with $G_{\alpha_j}^{(i)}$ substituted for $\sigma_{eq}^{(i)}$. The value of α_j that maximizes the log likelihood function is the best choice for statistical model $\mathcal{S}_1$ and the available calibration data.

In order to assess the relative merit of choosing α_j over α_1, given the statistical model $\mathcal{S}_1$ and the calibration data D, we compute the Bayes factors characterized by the parameter $\hat{\theta}_1$ (where $\theta = \{A_1\ A_2\ s\ \mu_f\ s_f\}$, see Section 2.3.1):

$$BF_j = \frac{\Pr\left(\mathrm{D} \mid G_{\alpha_j}, \hat{\theta}_1\right)}{\Pr\left(\mathrm{D} \mid G_{\alpha_1}, \hat{\theta}_1\right)} = \frac{L_j(\hat{\theta}_1)}{L_1(\hat{\theta}_1)} = \exp\left(LL_j(\hat{\theta}_1) - LL_1(\hat{\theta}_1)\right) \qquad \textbf{Eq. 32}$$

The results are shown in Table 4. The largest Bayes factor indicates the optimal choice for α, which are highlighted in red in the table.

Table 4: Bayes factors for Specimen #9

Material	β-fit	Bayers Factors for α						
		0.0	0.2	0.4	0.5	0.6	0.8	1.0
24S-T3	$(\beta)_{logN}$	1.00	6.30	39.38	96.75	230.30	**366.98**	16.22
	$(\beta)_{AVG}$	1.00	**4.50**	4.23	0.97	0.03	< 10^(-8)	< 10^(-27)
75S-T6	$(\beta)_{logN}$	1.00	1.62	15.45	61.88	420.8	17899	**8.00E+05**
	$(\beta)_{AVG}$	1.00	8.55	230.4	1252	**4477**	2792	0.01
SAE 4130	$(\beta)_{logN}$	**1.00**	0.021	4.9E-04	< 10^(-5)	<10^(-10)	<10^(-26)	<10^(-62)
	$(\beta)_{AVG}$	**1.00**	7.11E-14	******** Very small number ********				

The workflow for the selection of the optimal value of α described in Step 2 is summarized in Figure 14.

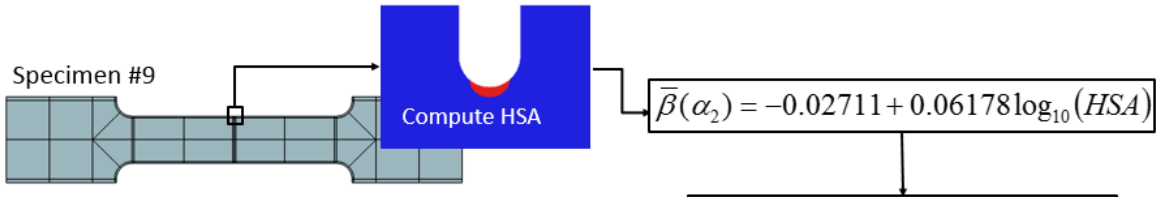

N	Failure	σ_{eq} (β) for α						
		0.0	0.2	0.4	0.5	0.6	0.8	1.0
8000	0	72.49	71.43	70.12	69.29	68.19	65.60	62.18
30000	0	57.99	57.14	56.10	55.44	54.55	52.48	49.74
104000	0	46.84	46.15	45.31	44.77	44.06	42.39	40.18
379000	0	35.69	35.17	34.52	34.11	33.57	32.30	30.61
760000	0	31.23	30.77	30.21	29.85	29.38	28.26	26.79
1096000	0	27.88	27.47	26.97	26.65	26.23	25.23	23.92
1287000	0	25.09	24.73	24.27	23.99	23.61	22.71	21.52
11390000	0	25.09	24.73	24.27	23.99	23.61	22.71	21.52
11226000	1	23.87	23.52	23.09	22.81	22.45	21.60	20.47
11281000	1	22.30	21.98	21.58	21.32	20.98	20.18	19.13
13420000	1	22.30	21.98	21.58	21.32	20.98	20.18	19.13
10000	0	58.33	57.48	56.43	55.76	54.88	52.79	50.04
18000	0	51.11	50.36	49.44	48.85	48.08	46.25	43.84
38500	0	43.71	43.07	42.28	41.78	41.12	39.55	37.49
114000	0	34.72	34.21	33.58	33.19	32.66	31.42	29.78
523000	0	24.94	24.57	24.12	23.84	23.46	22.57	21.39
10475000	1	16.73	16.48	16.18	15.99	15.74	15.14	14.35
Bayes factors:		1.00	6.30	39.38	96.75	230.30	**366.98**	16.22

Figure 14: Workflow for the selection of the optimal value of α.

Remark: The calibration of predictors can be considered reliable only if the numerical accuracy of the computed data is guaranteed. The values of the predictor reported herein were computed with StressCheck[2]. The relative errors, estimated by p-extension, were shown to be under 1%.

2.4.2 Summary of predictions

In this section we present a summary of the predictions for the optimal value of α for each material and for the two options used for the calibration of β as a function of the *HSA*. For each material, the summary includes the calibration data for the value of α that maximizes the log likelihood function when (a) the $\log_{10}\beta$ is assumed to be normally distributed, Eq. (30), and (b) fitting the arithmetic mean of β with a logarithmic fit, Eq. (31). The prediction of β for specimen #9 is shown in graphical form for both β-fits, together with the representation of the fatigue data on the reference S-N curve of the material. Finally the prediction of fatigue life based on the mean S-N curve, and the theoretical design curves associated with p = 1/1000 and p = 1/100000 are presented in tabular form.

2.4.2.1 Aluminum 24S-T3

Calibration data 24S-T3: Two optimal values of α are presented for the calibration of β as a function of the highly stressed area (*HSA*). As shown in Figure 15, α = 0.8 maximizes the log likelihood function when the $\log_{10}\beta$ is assumed to be normally distributed – Eq. (30), while α =

[2] StressCheck is a trademark of Engineering Software Research and Development, Inc.

0.2 maximizes the log likelihood function when fitting the arithmetic mean of β with a logarithmic fit – Eq. (31) – as shown in Figure 16.

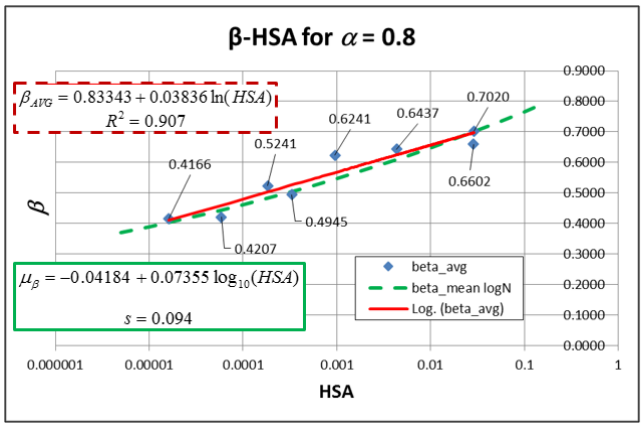

#	Specimen	β_{AVG}	β_{FIT}	β_{LogN}
2	Open Hole Kt=2.11	0.7020	0.6976	0.6999
8	Edge Notch r=0.760 in	0.6602	0.6973	0.6995
3	Edge Notch Kt=2.17	0.6437	0.6246	0.6085
4	Fillet Notch Kt=2.19	0.6241	0.5668	0.5446
10	Edge Notch r=0.071 in	0.4945	0.5262	0.5039
5	Edge Notch Kt=4.43	0.5241	0.5033	0.4822
7	Edge Notch Kt=5.83	0.4207	0.4598	0.4436
6	Fillet Notch Kt=4.83	0.4166	0.4103	0.4034

Figure 15: Calibration data for $\alpha = 0.8$ maximizes the log likelihood function when the $\log_{10}\beta$ is assumed to be normally distributed. Tabular data with the arithmetic average of β for each specimen type under the header β_{AVG}, the corresponding fitted value using the logarithmic fit of Eq. (31) under β_{FIT}, and the beta value from the linear regression fit of Eq. (30) under β_{LogN}. Aluminum 24S-T3.

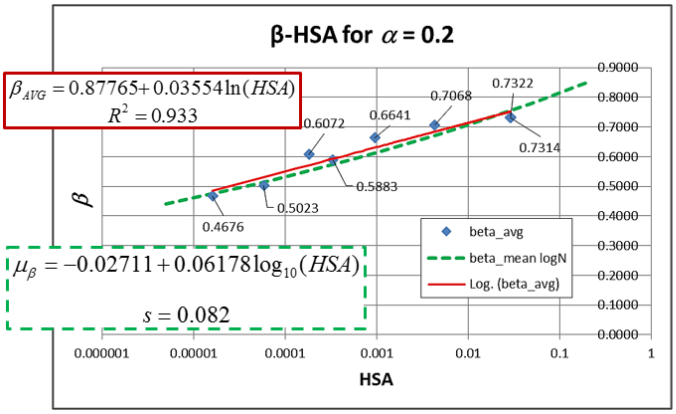

#	Specimen	β_{AVG}	β_{FIT}	β_{LogN}
2	Open Hole Kt=2.11	0.7314	0.7518	0.7549
8	Edge Notch r=0.760 in	0.7322	0.7515	0.7545
3	Edge Notch Kt=2.17	0.7068	0.6842	0.6712
4	Fillet Notch Kt=2.19	0.6641	0.6306	0.6114
10	Edge Notch r=0.071 in	0.5883	0.5930	0.5728
5	Edge Notch Kt=4.43	0.6072	0.5718	0.5520
7	Edge Notch Kt=5.83	0.5023	0.5315	0.5147
6	Fillet Notch Kt=4.83	0.4676	0.4856	0.4752

Figure 16: Calibration data for $\alpha = 0.2$ maximizes the log likelihood function when fitting the arithmetic mean of β with a logarithmic fit. Tabular data with the arithmetic average of β for each specimen type under the header β_{AVG}, the corresponding fitted value using the logarithmic fit of Eq. (31) under β_{FIT}, and the beta value from the linear regression fit of Eq. (30) under β_{LogN}. Aluminum 24S-T3.

Note that both curve fits are shown in each figure to illustrate how close they are to each other, even though only one is optimal in the sense of Eq. (32) for a given α. The box with solid lines over the equation indicates the expression of β for which the optimal value of α maximizes the log likelihood function, while the box with dotted lines over the equation indicates the fit done for the other expression of β for the same value of α. The tabular data show the values of the arithmetic average of β (heading β_{AVG}) for all 8 calibration specimens, the values of β obtained from Eq. (31) (heading β_{FIT}) and the values β obtained from Eq. (30) (heading β_{LogN}). Each of the last two columns in the table is boxed with the same color and line type as the corresponding equations in the graph.

Prediction of β for specimen #9 24S-T3: With the β-fit obtained from calibration, the value of β for the HSA of specimen #9 is predicted for each optimal value of α as shown in Figure 17 and Figure 18 for $\alpha = 0.8$ and $\alpha = 0.2$, respectively (see also Table 3). Additionally, the pair ($\sigma_{eq}(\beta)$, N) for each of the 17 tests available for specimen #9 are shown in the S-N curve of the material. Note that for each optimal value of α, one set of test points is more evenly distributed around the mean S-N curve than the other. In Figure 17 the open circles are closer to the mean S-N curve (β-fit from Eq. 30) and in Figure 18 the solid triangles are closer to the mean S-N curve (β-fit from Eq. 31).

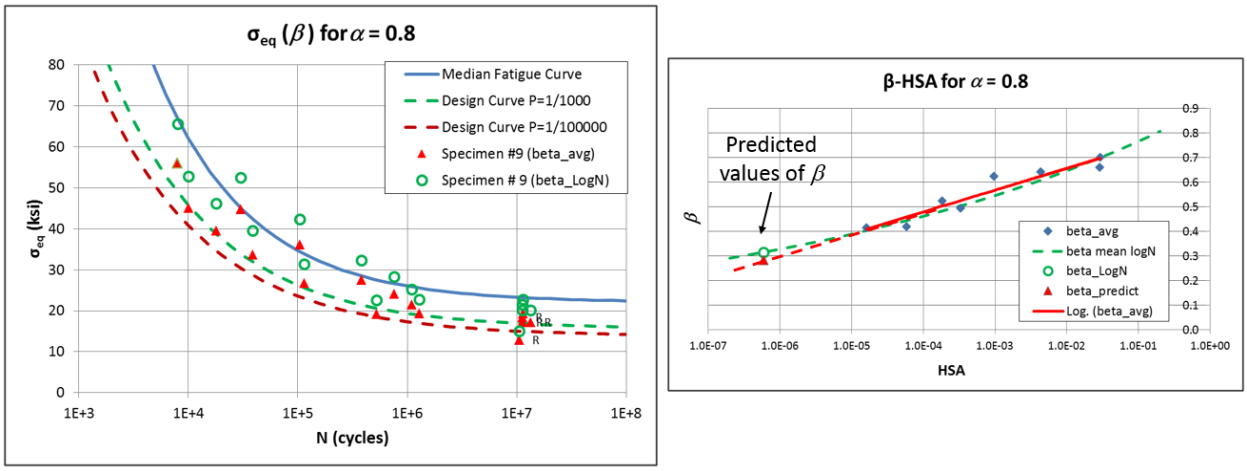

Figure 17: Predicted value of β for specimen #9 (right) and plot of the failed specimens on the reference S-N curve when σ_{eq} is computed from the predicted value of β (left). Aluminum 24S-T3 for $\alpha = 0.8$.

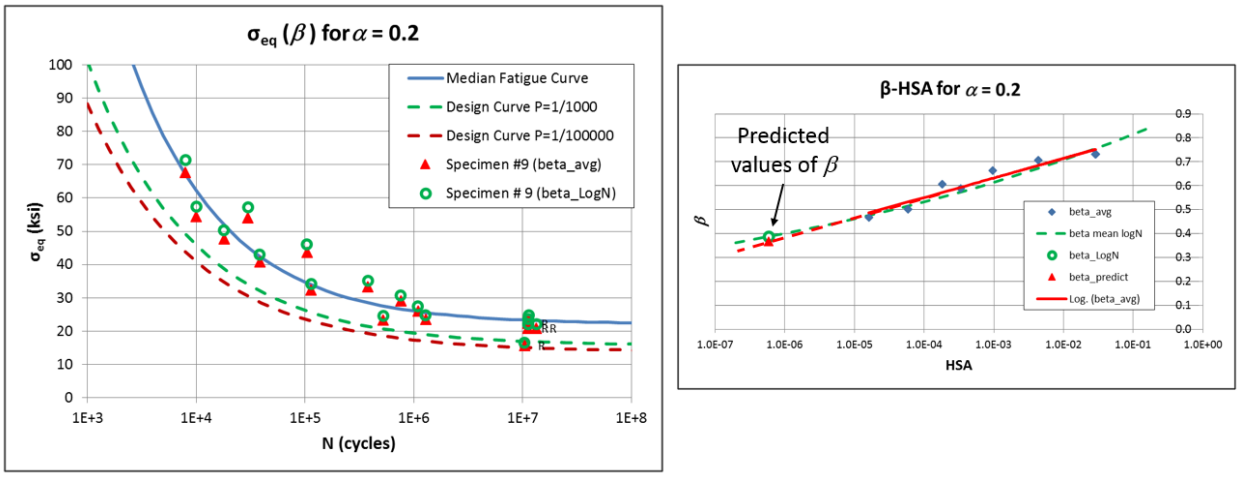

Figure 18: Predicted value of β for specimen #9 (right) and plot of the failed specimens on the reference S-N curve when σ_{eq} is computed from the predicted value of β (left). Aluminum 24S-T3 for $\alpha = 0.2$.

Life Prediction 24S-T3: The prediction of the number of cycles to failure for the 17 tests available for specimen #9 are shown in Table 5 for α = 0.8 and in Table 6 for α = 0.2, respectively. The second column shows the value of σ_{eq} (β) for each test, the next three prediction columns show the mean prediction based on the S-N curve of the material, and the predictions based on the theoretical design curves with P = 1/1,000 and with P = 1/100,000 using statistical model 1(see Figure 2). The next column shows the actual fatigue life recorded during the test (runouts are highlighted in red), and the last column in the table shows a "yes" if the predicted number of cycles to failure using the theoretical design curve with P = 1/1,000 is larger than the actual fatigue life.

Table 5: Prediction of the number of cycles to failure for specimen #9. Material 24S-T3, α = 0.8, β-fit Eq. (30)

#	Seq (ksi)	Prediction of N			Actual Fatigue Life	Over Prediction P=1/1000
		Mean	Design curve P=1/1000	Design Curve P=1/100000		
1	65.60	8,479	3,285	2,281	8,000	no
2	52.48	17,319	6,438	4,426	30,000	no
3	42.39	38,661	13,055	8,788	104,000	no
4	32.30	151,652	37,146	23,590	379,000	no
5	28.26	411,846	68,526	41,219	760,000	no
6	25.23	1,565,370	125,482	70,186	1,096,000	no
7	22.71	37,023,383	245,855	123,428	1,287,000	no
8	22.71	37,023,383	245,855	123,428	11,390,000	no
9	21.60	100,000,000	358,139	166,792	11,226,000	no
10	20.18	100,000,000	649,572	262,075	11,281,000	no
11	20.18	100,000,000	649,572	262,075	13,420,000	no
12	52.79	16,974	6,320	4,346	10,000	no
13	46.25	27,342	9,694	6,593	18,000	no
14	39.55	52,139	16,718	11,136	38,500	no
15	31.42	181,364	41,868	26,344	114,000	no
16	22.57	60,273,340	256,979	127,952	523,000	no
17	15.14	100,000,000	100,000,000	8,716,786	10,475,000	no

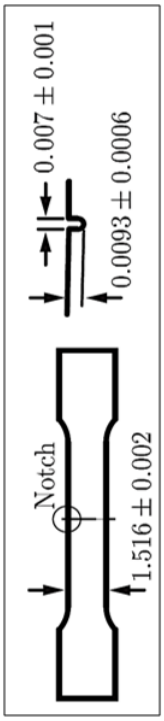

Table 6: Prediction of the number of cycles to failure for specimen #9. Material 24S-T3, $\alpha = 0.2$, β-fit Eq. (31)

#	Seq (ksi)	Prediction of N			Actual Fatigue Life	Over Prediction P=1/1000
		Mean	Design curve P=1/1000	Design Curve P=1/100000		
1	67.62	7,746	3,009	2,091	8,000	no
2	54.10	15,621	5,855	4,033	30,000	no
3	43.69	34,149	11,750	7,940	104,000	no
4	33.29	126,054	32,679	20,947	379,000	no
5	29.13	316,949	59,145	36,102	760,000	no
6	26.01	1,011,267	105,667	60,466	1,096,000	no
7	23.41	8,605,444	199,689	104,010	1,287,000	no
8	23.41	8,605,444	199,689	104,010	11,390,000	no
9	22.26	372,052,934	283,655	138,581	11,226,000	no
10	20.81	100,000,000	489,913	212,407	11,281,000	no
11	20.81	100,000,000	489,913	212,407	13,420,000	no
12	54.42	15,316	5,749	3,961	10,000	no
13	47.67	24,394	8,767	5,980	18,000	no
14	40.77	45,592	14,980	10,026	38,500	no
15	32.38	149,057	36,711	23,334	114,000	no
16	23.26	10,794,393	208,149	107,651	523,000	no
17	15.61	100,000,000	100,000,000	4,482,878	10,475,000	no

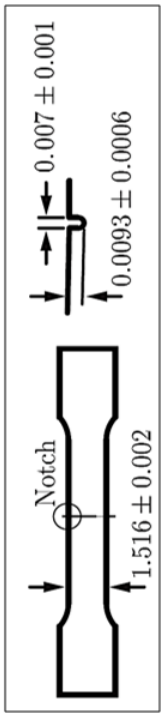

2.4.2.2 Aluminum 75S-T6

Calibration data 75S-T6: Two optimal values of α are presented for the calibration of β as a function of the highly stressed area (*HSA*). As shown in Figure 19, $\alpha = 1.0$ maximizes the log likelihood function when the $\log_{10}\beta$ is assumed to be normally distributed – Eq. (30), while $\alpha = 0.6$ maximizes the log likelihood function when fitting the arithmetic mean of β with a logarithmic fit – Eq. (31) – as shown in Figure 20.

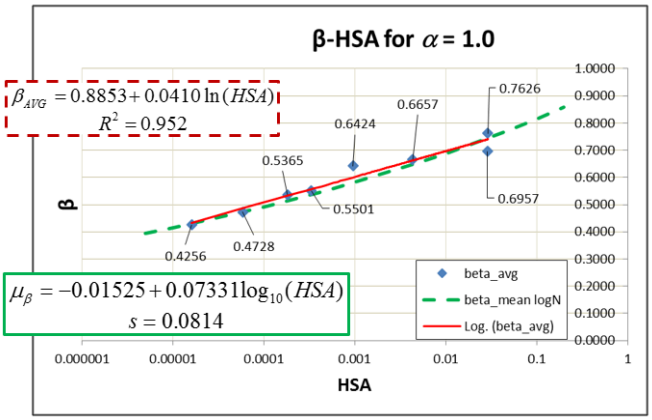

#	Specimen	β_{AVG}	β_{FIT}	β_{LogN}
2	Open Hole Kt=2.11	0.7626	0.7402	0.7448
8	Edge Notch r=0.760 in	0.6957	0.7398	0.7443
3	Edge Notch Kt=2.17	0.6657	0.6622	0.6478
4	Fillet Notch Kt=2.19	0.6424	0.6003	0.5800
10	Edge Notch r=0.071 in	0.5501	0.5570	0.5367
5	Edge Notch Kt=4.43	0.5365	0.5325	0.5137
7	Edge Notch Kt=5.83	0.4728	0.4861	0.4728
6	Fillet Notch Kt=4.83	0.4256	0.4331	0.4301

Figure 19: Calibration data for $\alpha = 1.0$ maximizes the log likelihood function when the $\log_{10}\beta$ is assumed to be normally distributed. Tabular data with the arithmetic average of β for each specimen type under the

header β_{AVG}, the corresponding fitted value using the logarithmic fit of Eq. (31) under β_{FIT}, and the beta value from the linear regression fit of Eq. (30) under β_{LogN}. Aluminum 75S-T6.

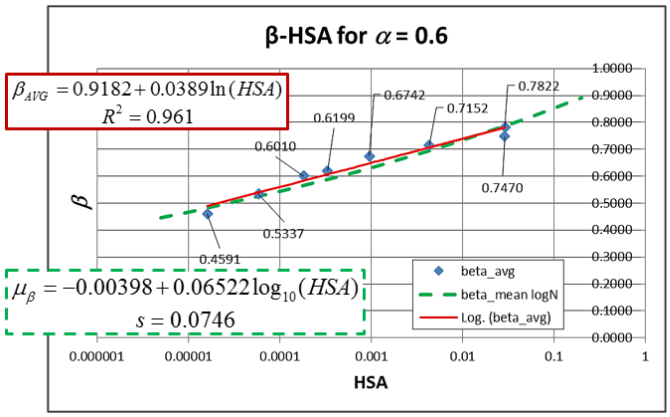

#	Specimen	β_{AVG}	β_{FIT}	β_{LogN}
2	Open Hole Kt=2.11	0.7822	0.7804	0.7865
8	Edge Notch r=0.760 in	0.7470	0.7801	0.7861
3	Edge Notch Kt=2.17	0.7152	0.7064	0.6948
4	Fillet Notch Kt=2.19	0.6742	0.6476	0.6296
10	Edge Notch r=0.071 in	0.6199	0.6065	0.5877
5	Edge Notch Kt=4.43	0.6010	0.5832	0.5652
7	Edge Notch Kt=5.83	0.5337	0.5391	0.5250
6	Fillet Notch Kt=4.83	0.4591	0.4889	0.4826

Figure 20: Calibration data for $\alpha = 0.6$ maximizes the log likelihood function when fitting the arithmetic mean of β with a logarithmic fit. Tabular data with the arithmetic average of β for each specimen type under the header β_{AVG}, the corresponding fitted value using the logarithmic fit of Eq. (31) under β_{FIT}, and the beta value from the linear regression fit of Eq. (30) under β_{LogN}. Aluminum 75S-T6.

As before, both curve fits are shown in each figure to illustrate how close they are to each other, even though only one is optimal in the sense of Eq. (32) for a given α. The box with solid lines over the equation indicates the expression of β for which the optimal value of α maximizes the log likelihood function, while the box with dotted lines over the equation indicates the fit done for the other expression of β for the same value of α. The tabular data show the values of the arithmetic average of β (heading β_{AVG}) for all 8 calibration specimens, the values of β obtained from Eq. (31) (heading β_{FIT}) and the values β obtained from Eq. (30) (heading β_{LogN}). Each of the last two columns in the table is boxed with the same color and line type as the corresponding equations.

Prediction of β for specimen #9 75S-T6: With the β-fit obtained from calibration, the value of β for the HSA of specimen #9 is predicted for each optimal value of α as shown in Figure 21 and Figure 22 for $\alpha = 1.0$ and $\alpha = 0.6$, respectively (see also Table 3). Additionally, the pair (σ_{eq} (β), N) for each of the 17 tests available for specimen #9 are shown in the S-N curve of the material. Note that for each optimal value of α, one set of test points is more evenly distributed around the mean than the other. In Figure 21 the open circles are closer to the mean S-N curve (β-fit from Eq. 30) and in Figure 22 the solid triangles are closer to the mean S-N curve (β-fit from Eq. 31).

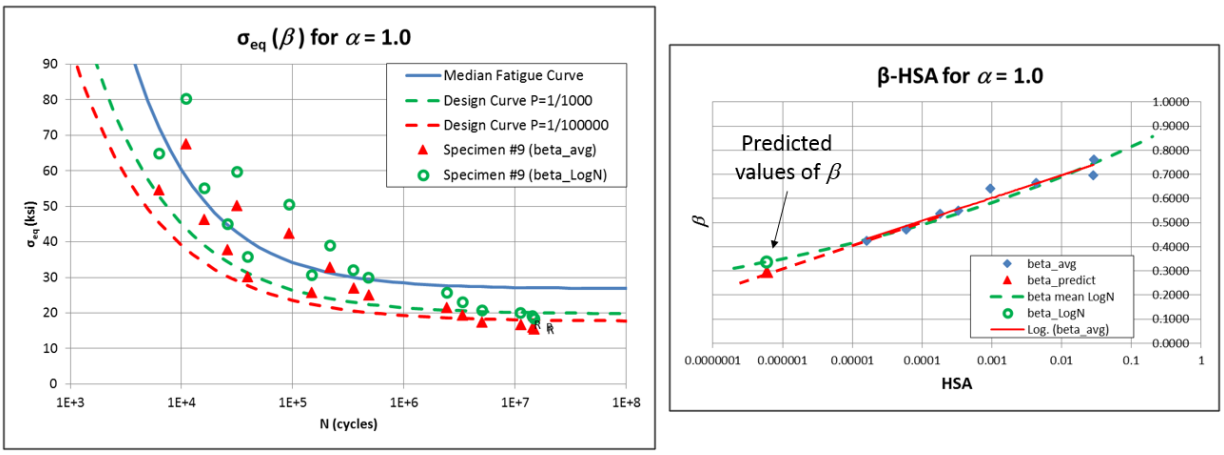

Figure 21: Predicted value of β for specimen #9 (right) and plot of the failed specimens on the reference S-N curve when σ_{eq} is computed from the predicted value of β (left). Aluminum 75S-T6 for α = 1.0.

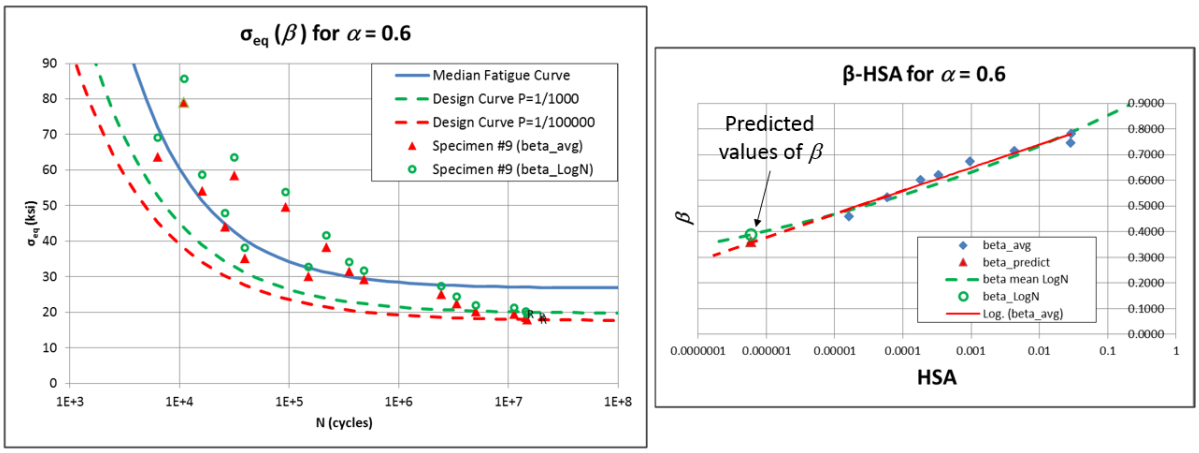

Figure 22: Predicted value of β for specimen #9 (right) and plot of the failed specimens on the reference S-N curve when σ_{eq} is computed from the predicted value of β (left). Aluminum 75S-T6 for α = 0.6.

Life Prediction75S-T6: The prediction of the number of cycles to failure for the 17 tests available for specimen #9 are shown in Table 7 for α = 1.0 and in Table 8 for α = 0.6, respectively. The second column shows the value of σ_{eq} (β) for each test, the next three prediction columns show the mean prediction based on the S-N curve of the material, and the predictions based on the theoretical design curves with P = 1/1,000 and with P = 1/100,000 using statistical model 1(see Figure 2). The next column shows the actual fatigue life recorded during the test (runouts are highlighted in red), and the last column in the table shows a "yes" if the predicted number of cycles to failure using the theoretical design curve with P = 1/1,000 is larger than the actual fatigue life. Note that only for test #8 in Table 8 the prediction of the number of cycles to failure (6,899,204) is larger than the actual fatigue life (5,045,000).

Table 7: Prediction of the number of cycles to failure for specimen #9. Material 75S-T6, α = 1.0, β-fit Eq. (30)

#	Seq (ksi)	Prediction of N			Actual Fatigue Life	Over Prediction P=1/1000
		Mean	Design curve P=1/1000	Design Curve P=1/100000		
1	80.32	4,892	2,211	1,463	11,000	no
2	59.67	10,319	4,557	2,999	31,500	no
3	50.49	17,034	7,170	4,668	93,000	no
4	39.01	46,937	16,115	10,096	217,000	no
5	32.13	166,847	34,644	20,287	353,000	no
6	29.83	394,392	49,379	27,644	482,000	no
7	22.95	100,000,000	355,396	122,821	3,375,000	no
8	20.65	100,000,000	2,963,171	338,536	5,045,000	no
9	19.97	100,000,000	26,565,547	538,306	11,299,000	no
10	18.36	100,000,000	100,000,000	4,348,178	14,874,000	no
11	64.91	8,227	3,679	2,428	6,300	no
12	55.11	12,966	5,623	3,685	16,000	no
13	44.97	25,559	10,104	6,493	26,000	no
14	35.82	74,573	22,048	13,494	39,500	no
15	30.69	269,378	42,863	24,460	149,000	no
16	25.66	100,000,000	124,145	58,649	2,441,000	no
17	19.03	100,000,000	100,000,000	1,347,182	14,390,000	no

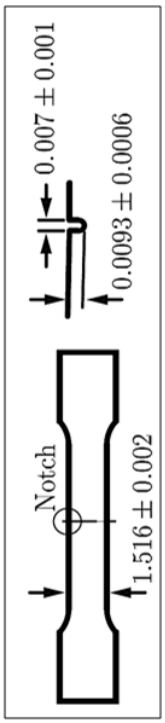

Table 8: Prediction of the number of cycles to failure for specimen #9. Material 75S-T6, α = 0.6, β-fit Eq. (31)

#	Seq (ksi)	Prediction of N			Actual Fatigue Life	Over Prediction P=1/1000
		Mean	Design curve P=1/1000	Design Curve P=1/100000		
1	78.88	5,100	2,305	1,525	11,000	no
2	58.60	10,854	4,777	3,141	31,500	no
3	49.58	18,080	7,551	4,907	93,000	no
4	38.31	51,363	17,180	10,717	217,000	no
5	31.55	198,674	37,616	21,817	353,000	no
6	29.30	529,988	54,247	29,958	482,000	no
7	22.54	100,000,000	449,293	141,899	3,375,000	no
8	20.28	100,000,000	6,899,204	427,885	5,045,000	yes
9	19.61	100,000,000	100,000,000	725,382	11,299,000	no
10	18.03	100,000,000	100,000,000	12,735,275	14,874,000	no
11	63.75	8,627	3,850	2,539	6,300	no
12	54.12	13,689	5,906	3,866	16,000	no
13	44.17	27,395	10,688	6,851	26,000	no
14	35.18	83,476	23,658	14,393	39,500	no
15	30.14	339,824	46,855	26,423	149,000	no
16	25.20	100,000,000	142,696	65,196	2,441,000	no
17	18.69	100,000,000	100,000,000	2,221,527	14,390,000	no

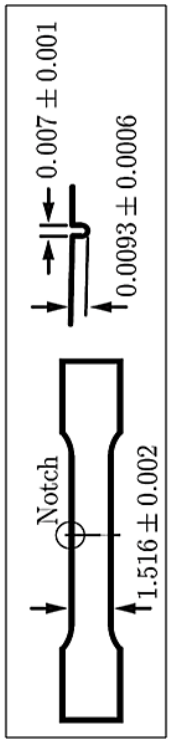

2.4.2.3 Steel SAE 4130

Calibration data SAE 4130: For this material, one value of α was found to be optimal for the calibration of β as a function of the highly stressed area (*HSA*). As shown in Figure 23, $\alpha = 0.0$ maximizes the log likelihood function when the $\log_{10} \beta$ is assumed to be normally distributed – Eq. (30) – and when fitting the arithmetic mean of β with a logarithmic fit – Eq. (31).

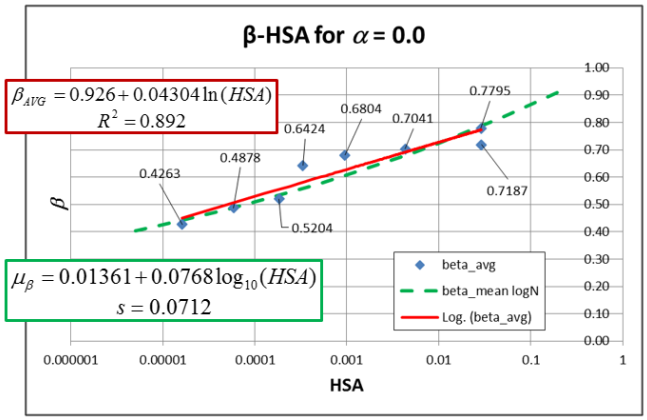

Specimen	β_{AVG}	β_{FIT}	β_{LogN}
Open Hole Kt=2.11	0.7187	0.7735	0.7862
Edge Notch r=0.760 in	0.7795	0.7732	0.7857
Edge Notch Kt=2.17	0.7041	0.6917	0.6793
Fillet Notch Kt=2.19	0.6804	0.6267	0.6050
Edge Notch r=0.071 in	0.6424	0.5812	0.5578
Edge Notch Kt=4.43	0.5204	0.5555	0.5328
Edge Notch Kt=5.83	0.4878	0.5067	0.4884
Fillet Notch Kt=4.83	0.4263	0.4511	0.4423

Figure 23: Calibration data for $\alpha = 0.0$ maximizes the log likelihood function for both forms of β fitting. Tabular data with the arithmetic average of β for each specimen type under the header β_{AVG}, the corresponding fitted value using the logarithmic fit of Eq. (31) under β_{FIT}, and the beta value from the linear regression fit of Eq. (30) under β_{LogN}. Steel SAE 4130.

Note that both curve fits shown in the figure are boxed with solid lines over the equation since both expressions of β are optimal for the same value of α. The tabular data show the values of the arithmetic average of β (heading β_{AVG}) for all 8 calibration specimens, the values of β obtained from Eq. (31) (heading β_{FIT}) and the values β obtained from Eq. (30) (heading β_{LogN}). Each of the last two columns in the table is boxed with the same color and line type as the corresponding equations.

Prediction of β for specimen #9 SAE 4130: With the β-fit obtained from calibration, the value of β for the HSA of specimen #9 is predicted for the optimal value of α as shown in Figure 21 for $\alpha = 0.0$ (see also Table 3). Additionally, the pair (σ_{eq} (β), N) for each of the 16 tests available for specimen #9 are shown in the S-N curve of the material. The open circles were determined for the β-fit given by Eq. 30 and the solid triangles from the β-fit from Eq. 31.

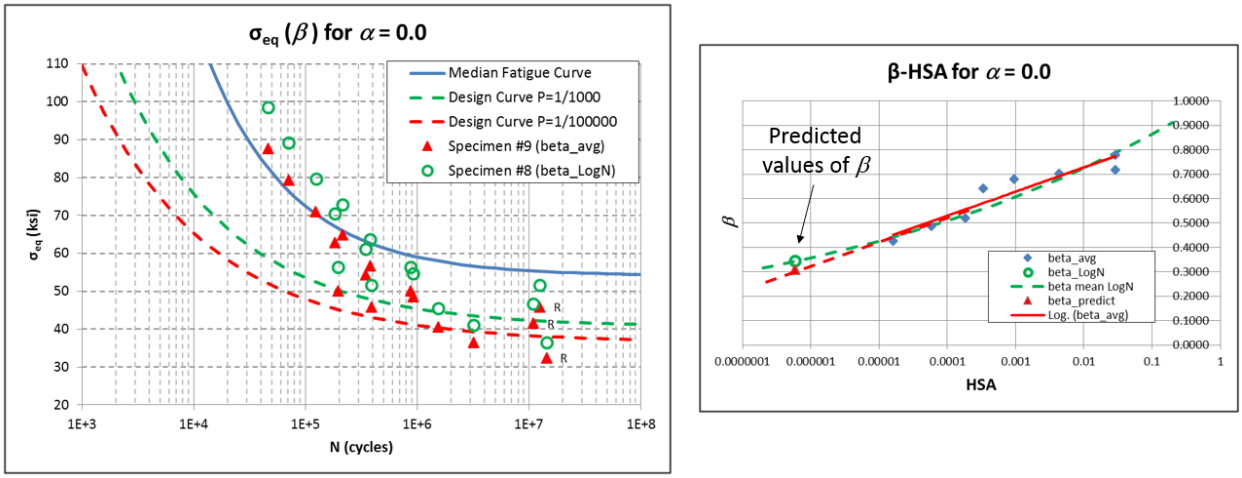

Figure 24: Predicted value of β for specimen #9 (right) and plot of the failed specimens on the reference S-N curve when σ_{eq} is computed from the predicted value of β (left). Steel SAE 4130 for $\alpha = 0.0$.

Life Prediction SAE 4130: The prediction of the number of cycles to failure for the 16 tests available for specimen #9 are shown in Table 9 when β-fit given by Eq. 30 and in Table 10 when the β-fit given by Eq. 31, both for $\alpha = 0.0$. The second column shows the value of $\sigma_{eq}(\beta)$ for each test, the next three prediction columns show the mean prediction based on the S-N curve of the material, and the predictions based on the theoretical design curves with P = 1/1,000 and with P = 1/100,000 using statistical model 1(see Figure 2). The next column shows the actual fatigue life recorded during the test (runouts are highlighted in red), and the last column in the table shows a "yes" if the predicted number of cycles to failure using the theoretical design curve with P = 1/1,000 is larger than the actual fatigue life. Note that only for test #6 in Table 9 the prediction of the number of cycles to failure (330,840,339) is larger than the actual fatigue life (3,193,000), while for tests #12 and #14 in Table 10 the predicted numbers of cycles to failure are larger than the actual fatigue life (206.229 > 195,000 for #12 and 824,410 > 389,000 for #14).

Table 9: Prediction of the number of cycles to failure for specimen #9. Steel SAE 4130, $\alpha = 0.0$, β-fit Eq. (30)

#	Seq (ksi)	Prediction of N			Actual Fatigue Life	Over Prediction P=1/1000
		Mean	Design curve P=1/1000	Design Curve P=1/100000		
1	79.71	55,355	7,763	3,674	124,000	no
2	72.88	95,664	12,115	5,631	215,000	no
3	63.77	308,205	26,130	11,515	379,000	no
4	54.66	45,449,762	83,187	31,589	919,000	no
5	45.55	100,000,000	935,777	178,161	1,546,000	no
6	41.00	100,000,000	330,840,339	1,015,979	3,193,000	yes
7	36.44	100,000,000	100,000,000	100,000,000	14,394,000	no
8	98.54	20,948	3,122	1,498	46,000	no
9	89.26	31,662	4,679	2,239	71,000	no
10	70.57	120,624	14,395	6,629	182,000	no
11	61.11	542,964	34,660	14,853	347,000	no
12	56.34	4,033,665	64,014	25,352	195,000	no
13	56.34	4,033,665	64,014	25,352	874,000	no
14	51.53	100,000,000	149,014	50,494	389,000	no
15	51.53	100,000,000	149,014	50,494	12,508,000	no
16	46.68	100,000,000	582,073	133,160	10,950,000	no

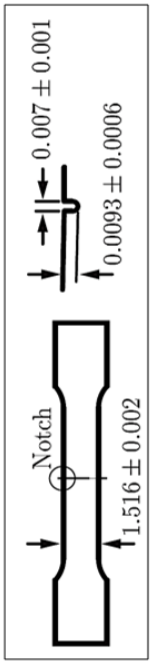

Table 10: Prediction of the number of cycles to failure for specimen #9. Steel SAE 4130, $\alpha = 0.0$, β-fit Eq. (31)

#	Seq (ksi)	Prediction of N			Actual Fatigue Life	Over Prediction P=1/1000
		Mean	Design curve P=1/1000	Design Curve P=1/100000		
1	70.89	116,590	14,044	6,477	124,000	no
2	64.81	257,408	23,600	10,493	215,000	no
3	56.71	3,090,802	60,683	24,224	379,000	no
4	48.61	100,000,000	306,757	86,437	919,000	no
5	40.51	100,000,000	100,000,000	1,353,097	1,546,000	no
6	36.46	100,000,000	100,000,000	100,000,000	3,193,000	no
7	32.41	100,000,000	100,000,000	100,000,000	14,394,000	no
8	87.63	34,427	5,064	2,420	46,000	no
9	79.38	56,659	7,920	3,746	71,000	no
10	62.75	374,889	28,997	12,654	182,000	no
11	54.35	186,773,493	87,668	32,989	347,000	no
12	50.10	100,000,000	206,229	64,720	195,000	yes
13	50.10	100,000,000	206,229	64,720	874,000	no
14	45.83	100,000,000	824,410	165,254	389,000	yes
15	45.83	100,000,000	824,410	165,254	12,508,000	no
16	41.51	100,000,000	47,955,657	776,663	10,950,000	no

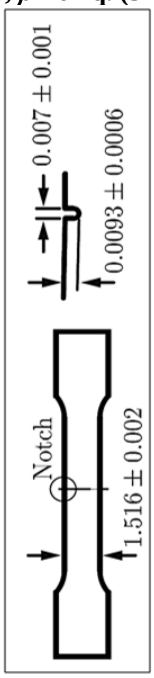

2.4.3 Validation of the predictions

The statement: "this model has been validated" should be understood to mean that one has a high degree of belief, supported by experimental evidence, that the model in question will perform its predictive function reliably. This statement is incomplete however without a qualifying statement concerning the range of parameters and range of data for which one believes the model has been validated.

We considered the formulation and calibration of a model characterized by two parameters α and β. We used a subset of the available data, the training set, to calibrate the parameter β for fixed values of α. We then used the remaining data, the validation set, to determine optimal values for α. In the calibration process the model is assumed to be correct and β_i, corresponding to the training data, are determined by projecting each data point onto the S-N curve by means of Eq. (29). We calibrated the model for each α. We then considered ranking the models with respect to the validation set based on specimen #9.

As shown in Figure 17 for aluminum 24S-T3 (α = 0.8), the predicted values of β fall outside the range of the training set (the same is true for the other materials and for different values of α). We then updated the training set to include the validation set and obtained a new calibration curve β – *HSA* for each material and for the optimal values of α corresponding to the β-fits using Eq. (30) and Eq. (31). The updated calibration curves are shown in Figure 25 to Figure 29.

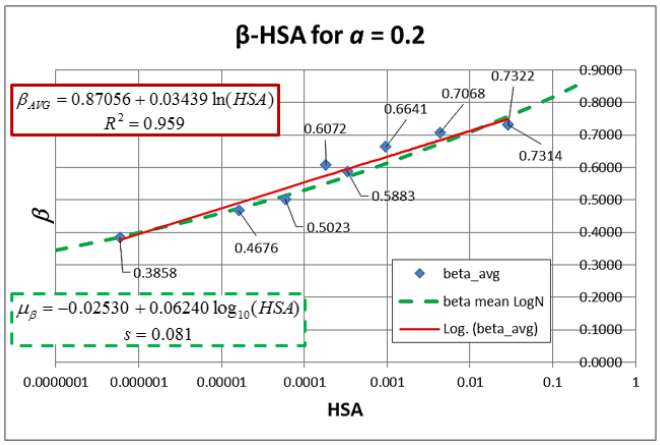

#	Specimen	β_{AVG}	β_{FIT}	β_{LogN}
2	Open Hole Kt=2.11	0.7314	0.7488	0.7564
8	Edge Notch r=0.760 in	0.7322	0.7485	0.7560
3	Edge Notch Kt=2.17	0.7068	0.6834	0.6717
4	Fillet Notch Kt=2.19	0.6641	0.6314	0.6113
10	Edge Notch r=0.071 in	0.5883	0.5951	0.5723
5	Edge Notch Kt=4.43	0.6072	0.5745	0.5514
7	Edge Notch Kt=5.83	0.5023	0.5356	0.5137
6	Fillet Notch Kt=4.83	0.4676	0.4911	0.4740
9	Edge Notch r=0.0035	0.3858	0.3773	0.3855

Figure 25: Updated β calibration for α = 0.2 including all 9 specimen types. Aluminum 24S-T3.

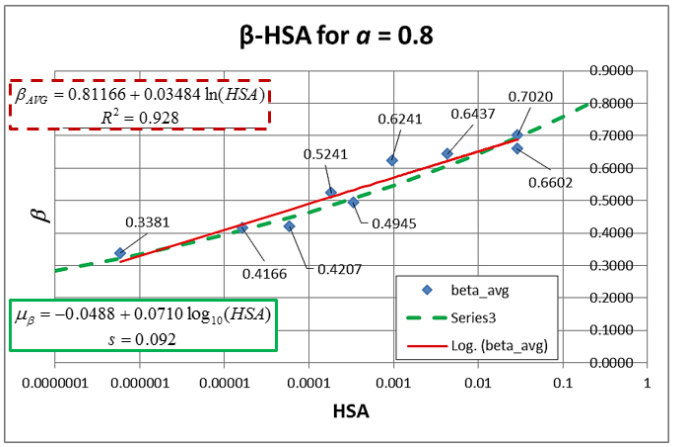

#	Specimen	β_{AVG}	β_{FIT}	β_{LogN}
2	Open Hole Kt=2.11	0.7020	0.6883	0.6950
8	Edge Notch r=0.760 in	0.6602	0.6880	0.6946
3	Edge Notch Kt=2.17	0.6437	0.6220	0.6072
4	Fillet Notch Kt=2.19	0.6241	0.5695	0.5455
10	Edge Notch r=0.071 in	0.4945	0.5327	0.5061
5	Edge Notch Kt=4.43	0.5241	0.5118	0.4851
7	Edge Notch Kt=5.83	0.4207	0.4724	0.4476
6	Fillet Notch Kt=4.83	0.4166	0.4274	0.4083
9	Edge Notch r=0.0035 in	0.3381	0.3121	0.3228

Figure 26: Updated β calibration for $\alpha = 0.8$ including all 9 specimen types. Aluminum 24S-T3.

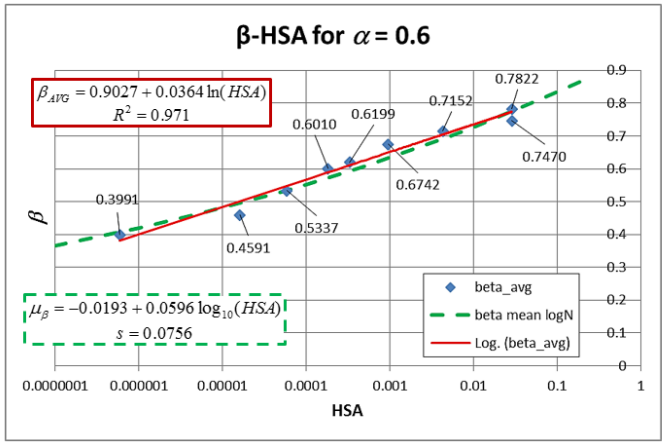

#	Specimen	β_{AVG}	β_{FIT}	β_{LogN}
2	Open Hole Kt=2.11	0.7822	0.7738	0.7745
8	Edge Notch r=0.760 in	0.7470	0.7735	0.7742
3	Edge Notch Kt=2.17	0.7152	0.7045	0.6915
4	Fillet Notch Kt=2.19	0.6742	0.6496	0.6320
10	Edge Notch r=0.071 in	0.6199	0.6111	0.5935
5	Edge Notch Kt=4.43	0.6010	0.5893	0.5727
7	Edge Notch Kt=5.83	0.5337	0.5481	0.5353
6	Fillet Notch Kt=4.83	0.4591	0.5010	0.4956
9	Edge Notch r=0.0035 in	0.3991	0.3805	0.4069

Figure 27: Updated β calibration for $\alpha = 0.6$ including all 9 specimen types. Aluminum 75S-T6.

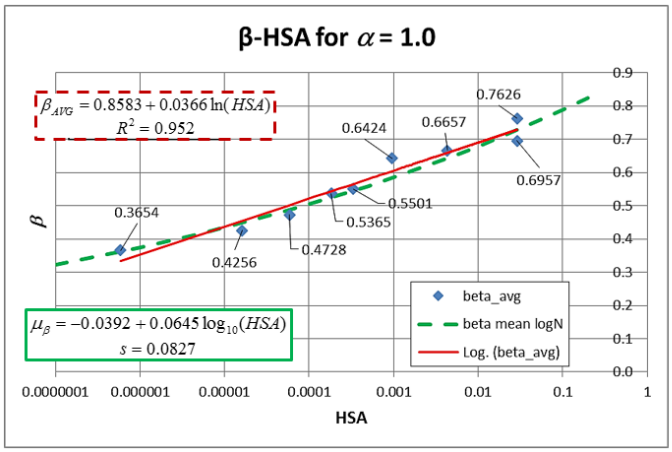

#	Specimen	β_{AVG}	β_{FIT}	β_{LogN}
2	Open Hole Kt=2.11	0.7626	0.7286	0.7271
8	Edge Notch r=0.760 in	0.6957	0.7283	0.7267
3	Edge Notch Kt=2.17	0.6657	0.6590	0.6432
4	Fillet Notch Kt=2.19	0.6424	0.6037	0.5835
10	Edge Notch r=0.071 in	0.5501	0.5650	0.5451
5	Edge Notch Kt=4.43	0.5365	0.5431	0.5244
7	Edge Notch Kt=5.83	0.4728	0.5016	0.4875
6	Fillet Notch Kt=4.83	0.4256	0.4543	0.4485
9	Edge Notch r=0.0035 in	0.3654	0.3331	0.3623

Figure 28: Updated β calibration for $\alpha = 1.0$ including all 9 specimen types. Aluminum 75S-T6.

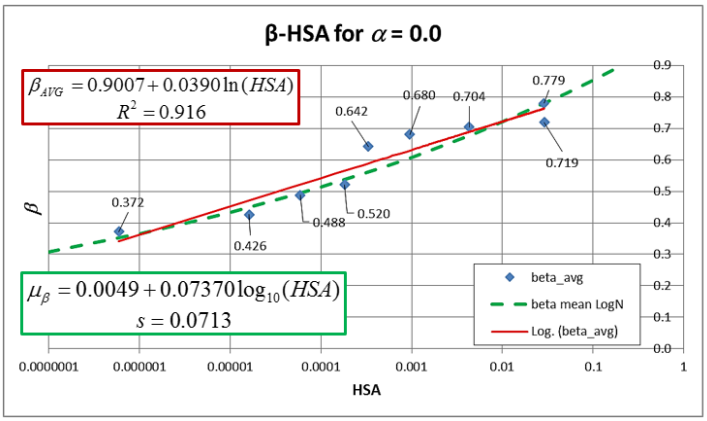

#	Specimen	β_{AVG}	β_{FIT}	β_{LogN}
2	Open Hole Kt=2.11	0.7187	0.7627	0.7790
8	Edge Notch r=0.760 in	0.7795	0.7624	0.7786
3	Edge Notch Kt=2.17	0.7041	0.6886	0.6771
4	Fillet Notch Kt=2.19	0.6804	0.6298	0.6058
10	Edge Notch r=0.071 in	0.6424	0.5887	0.5605
5	Edge Notch Kt=4.43	0.5204	0.5654	0.5363
7	Edge Notch Kt=5.83	0.4878	0.5212	0.4933
6	Fillet Notch Kt=4.83	0.4263	0.4709	0.4485
9	Edge Notch r=0.0035 i	0.3722	0.3420	0.3514

Figure 29: Updated β calibration for α = 0.0 including all 9 specimen types. Steel SAE 4130.

The data is also available in the Excel files: Calibration-All-(24S-T3-SWT)-RFL-Model-1-Alpha-02.xlsm; Calibration-All-(24S-T3-SWT)-RFL-Model-1-Alpha-08.xlsm; Calibration-All-(75S-T6-SWT)-RFL-Model-1-Alpha-06.xlsm; Calibration-All-(75S-T6-SWT)-RFL-Model-1-Alpha-10.xlsm; Calibration-All-SAE-4130-RFL-Model-1-Alpha-00.xlsm (see Appendix 4 for details).

We now state that

1. The model has been validated. Using statistical model 1 for characterizing the S-N data and two models to characterize the β – *HSA* relation for each material, we found the optimal values of α that maximizes the Bayes factors as shown in Table 11 (extracted from Table 4).

Table 11: Optimal value of α for each material and β-fit

Material	Optimal Value of α	
	$(\beta)_{logN}$	$(\beta)_{AVG}$
24S-T3	0.80	0.20
75S-T6	1.00	0.60
SAE 4130	0.00	0.00

2. The ranges of parameters and data for which validation is claimed are approximately $10^{-7} < \text{HSA} < 10^{-1}$ (in^2), $10^4 < N < 10^7$, $\mu - 2s < \log10\ N < \mu + 2s$ where s is the standard deviation.

2.4.4 Formulation of design rules

Design rules for structural and mechanical components subjected cyclic loading are stated in the form of a predictor and its allowable value.

The predictor considered herein depends on the material properties (because the parameter α depends on the material), its allowable value depends on both the material properties and the number of load cycles that the component is expected to endure. Incorporated in the allowable value is a factor of safety chosen to account for both aleatory and epistemic uncertainties. We distinguish between two kinds of epistemic uncertainties:

1. Model form uncertainties. These are uncertainties associated with the assumptions incorporated in the mathematical problem, the definition of the predictor and the definition of the statistical model.
2. Errors in the numerical solution. It must be verified that errors in the numerical solution of the mathematical model are within tight tolerances at all times. Otherwise model form uncertainties and numerical errors cannot be separated, making proper assessment and ranking of mathematical models impossible. Solution verification is an essential technical requirement of numerical simulation [9].

We have considered constant amplitude loading only. Additional epistemic uncertainties of the first kind are associated with the choice of cumulative fatigue damage models in variable amplitude loading. Ideally, epistemic uncertainties would be negligibly small in comparison with aleatory uncertainties.

2.5 Uncertainty Quantification

The aleatory uncertainties in β are correlated with the uncertainties in the S-N data. Since the S-N curve represents the mean fatigue life of the material, the mean value of β for a given G_α is one possible generalization for the notched specimens. We utilize the generalization of the mean value of β given by Eq. (30) as described in Section 2.4.1, which assumes that for a fixed *HSA*, $\log_{10}\beta$ is normally distributed with standard deviation s_β. Next we consider the mean value of β plus one standard deviation to quantify the uncertainty in the predicted fatigue life of Specimen #9.

The model-form uncertainty is associated with the selection of G_α. The selection of G_α depends on the model used for fitting the available data during calibration for determining the relation β – *HSA*. We utilize the optimal values of α obtained for the two generalizations of the mean value of β given by Eq. (30) and (31) to compute two values of G_α for the prediction of fatigue life of Specimen # 9.

Aluminum 24S-T3. Consider the quantification of the aleatory and model-form uncertainties associated with the prediction of fatigue life of specimen #9.

The predicted value of β for each optimal value of α identified in Section 2.4.1 and 2.4.2 was used to quantify one aspect of the model-form uncertainty in the prediction of the mean number of cycles to failure of test case 4 for which the actual fatigue life during the test was 379,000 cycles. As shown in Table 5 and Table 6, the predicted mean number of cycles to failure for the model based on $G_{0.8}$ (corresponding to the β-fit given by Eq. 30) is 151,652, while for the model based on $G_{0.2}$ (corresponding to the β-fit given by Eq. 31) is 126,054.

Quantification of uncertainty associated with the choice of fitting algorithm for β is summarized in Figure 30 for test case #4. For all other test cases the effect of model-form uncertainty in the prediction of the number of cycles to failure is realized by comparing the 'Prediction of N' columns of Table 5 and Table 6.

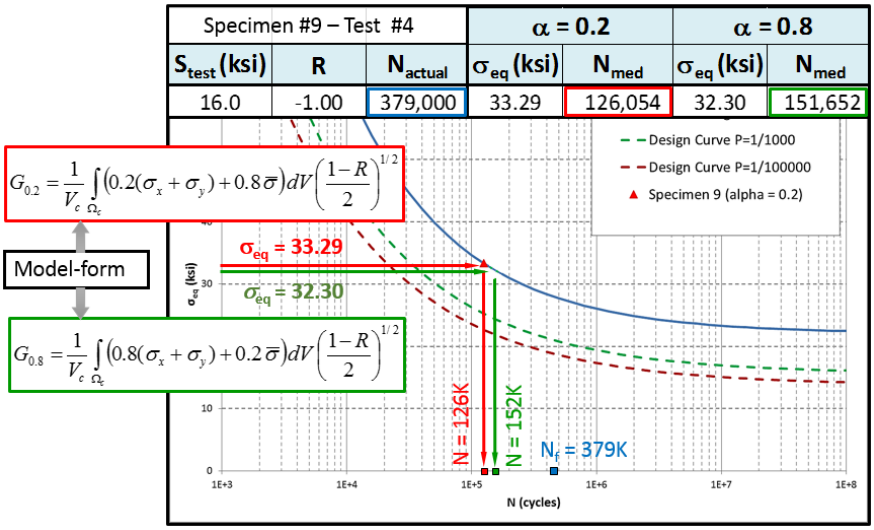

Figure 30: Quantification of uncertainty for associated with the selection of β for Specimen #9 - Test #4. Aluminum 24S-T3.

The quantification of aleatory uncertainty is illustrated with the determination of β for specimen #9 considering the mean of the β-fit given by Eq. (30) and the mean plus one standard deviation. As shown in Figure 31, the predicted values of β for each case are 0.3163 and 0.3925 for the mean curve fit and the mean plus one standard deviation, respectively.

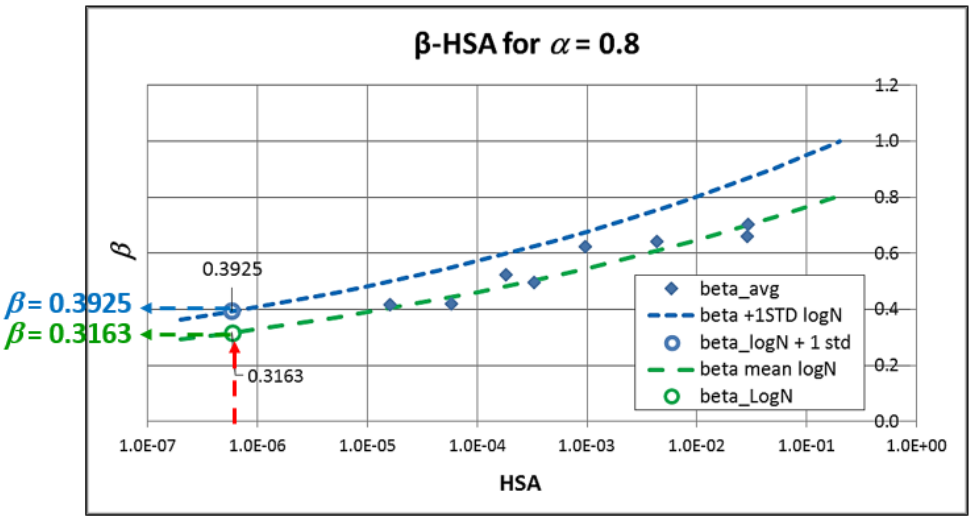

Figure 31: Predicted values of β for specimen #9 for the model characterized by $\alpha = 0.8$ from the mean β-*HAS* curve fit and the mean plus one standard deviation. Aluminum 24S-T3.

With the predicted values of β we now compute the G_α for test case 4 and the corresponding estimated number the cycles to failure using the mean S-N curve of the material:

$$\sigma_{eq} = G_{0.8} = \frac{1}{V_c}\int_{\Omega_c}\left(0.8\,I_1 + 0.2\,\overline{\sigma}\right)dV\left(\frac{1-R}{2}\right)^{1/2} \quad \text{with} \quad \Omega_c = \left\{\vec{x} \mid \sigma_1 \geq \beta\,\sigma_{peak}\right\}$$

$$\text{For } \beta = 0.316 \rightarrow \sigma_{eq} = 32.30 \text{ ksi}$$
$$\text{For } \beta = 0.392 \rightarrow \sigma_{eq} = 41.47 \text{ ksi}$$

Figure 32 shows the effect of the aleatory uncertainty in the prediction of fatigue life assuming that the model is correct. By model we understand the entire process by which predictions are made.

Specimen #9 – Test #4			$\alpha = 0.8, \beta_m$		$\alpha = 0.8, \beta_{m+1\,std}$	
S_{test} (ksi)	R	N_{actual}	σ_{eq} (ksi)	N_{med}	σ_{eq} (ksi)	N_{med}
16.0	-1.00	379,000	32.3	151,652	41.47	42,380

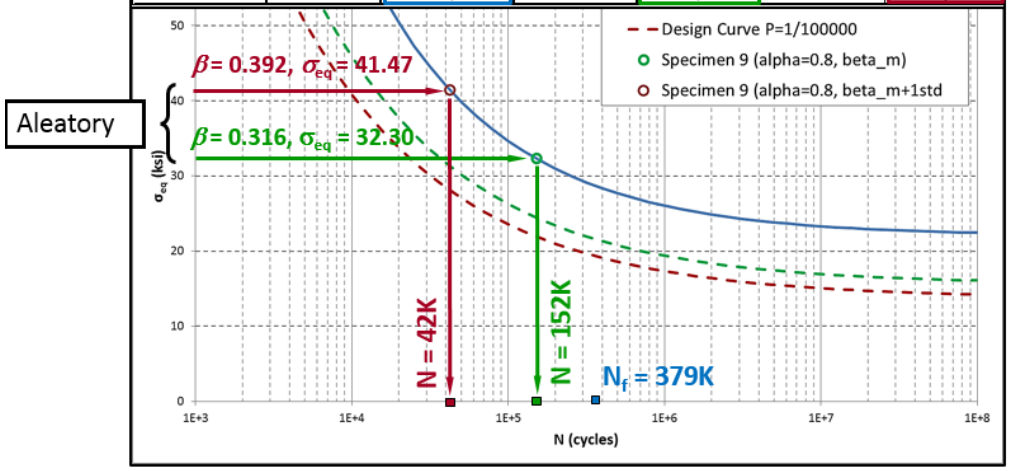

Figure 32: Quantification of aleatory uncertainty for Specimen #9 - Test #4. Aluminum 24S-T3.

Steel SAE 4130. Consider the quantification of the model-form uncertainty associated with the prediction of the mean number of cycles to failure for specimen #9 of steel. In this case we look at the prediction for test cases #2 and #10 shown in Table 9 and Table 10 when, for the same optimal values of $\alpha = 0$, the value of β is given by Eq. (30) or (31) in the computation of $G_{\alpha=0}$.

These specimens were tested a different stress levels (S_{test} = 40 ksi and S_{test} = 50 ksi for #2 and #10, respectively) and load ratios (R = −1.0 and R = −0.2, for #2 and #10 respectively), but they have very similar equivalent stress, and therefore the expected life should also be similar. The effect of the model-form uncertainty in the prediction is summarized in Figure 33.

Specimen #9 – Tests #2 & #10				β_{FIT}		β_{LogN}	
#	S_{test} (ksi)	R	N_{actual}	σ_{eq} (ksi)	N_{med}	σ_{eq} (ksi)	N_{med}
2	40.0	-1.00	215,000	64.81	257,408	72.88	95,664
10	50.0	-0.20	182,000	62.75	374,889	70.57	120,624

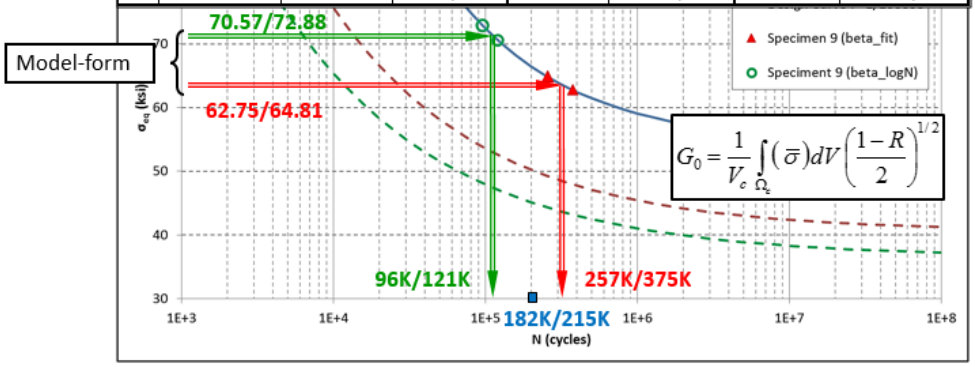

Figure 33: Quantification of model-form uncertainty for Specimen #9 - Tests #2 and #10. Steel SAE 4130.

2.5.1 Frequency plots

In Section 2.4.1, it was assumed that for a fixed value of the highly stressed area (*HSA*), $\log_{10}\beta$ is normally distributed and that the mean (μ_β) is a linear function of $\log_{10}$ *HSA* with constant standard deviation s_β. In order to check this assumption, a frequency plot was constructed for the optimal value of α for each material.

Figure 42 shows the calibration curve of β for aluminum 24S-T3 for α = 0.8. The symbols correspond to the computed values of β for each test case of the 8 specimen types used for calibration shown in Table 2. The dotted line is the estimate of the mean value of β as a function of the *HSA* determined from Eq. (30):

$$\mu_\beta = -0.04184 + 0.07355\log_{10}(HSA), \text{ with } s_\beta = 0.094$$

The Z-score measures how many standard deviations each point β_i is from the mean μ_β. The Z-score is defined as:

$$Z_i = \frac{\log_{10}\beta_i - \mu_\beta}{s_\beta} \qquad \textbf{Eq. 33}$$

The groupings of the Z-scores in bins form the frequency plot. The data is available in the Excel file: BetaZ-Score-Alpha-0.8(24S-T3).xlsx and summarized in Figure 35 to Figure 37 for each specimen type and for all specimens combined. Since specimens 2 and 8 have practically the same *HSA* (see Table 2), a single frequency plot was prepared for both. The results clearly show that the log-normal distribution assumption is supported by the resulting distribution in the frequency plots.

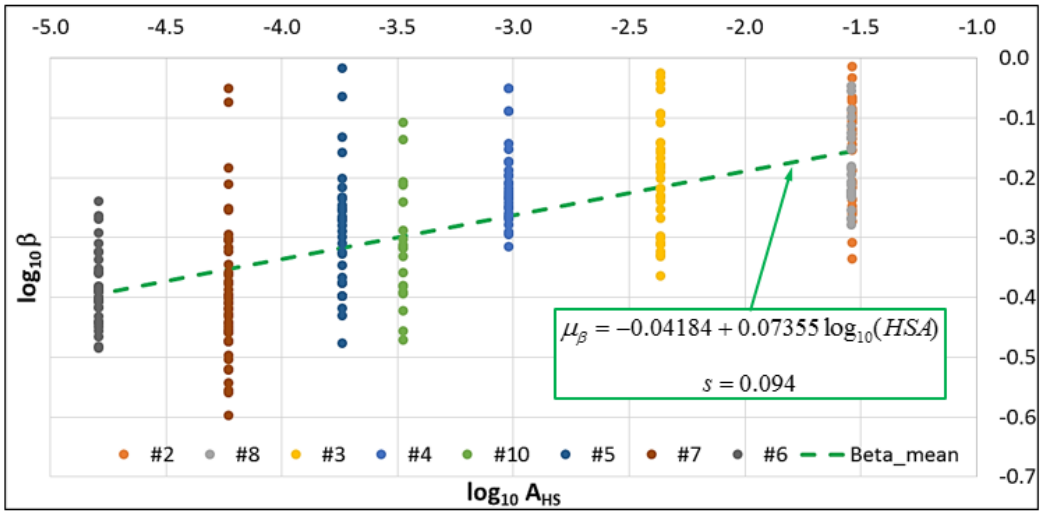

Figure 34: Calibration curve for β, aluminum 24S-T3 and α = 0.8. Symbols are the computed values of β for each specimen type (Section 2.4.1), and the dotted line is the fit of the mean value of β.

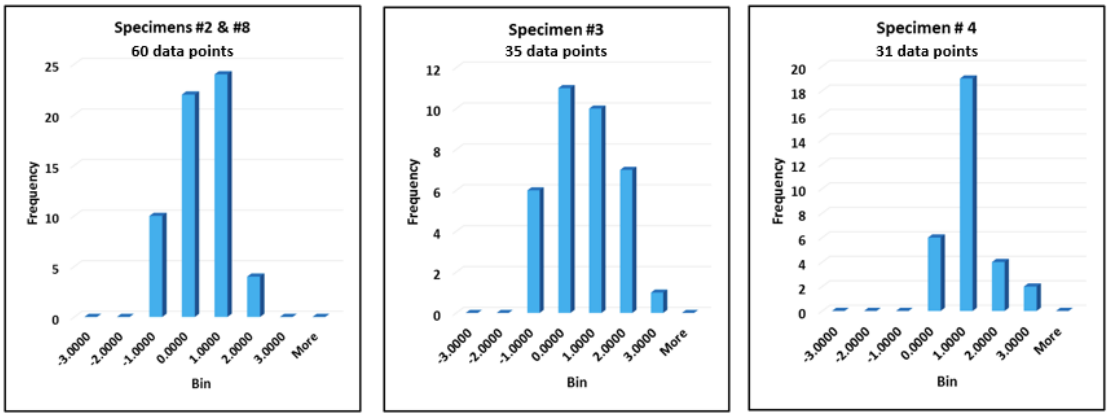

Figure 35: Frequency plot for specimen types 2 & 8 combined, 3 and 4. Aluminum 24S-T3.

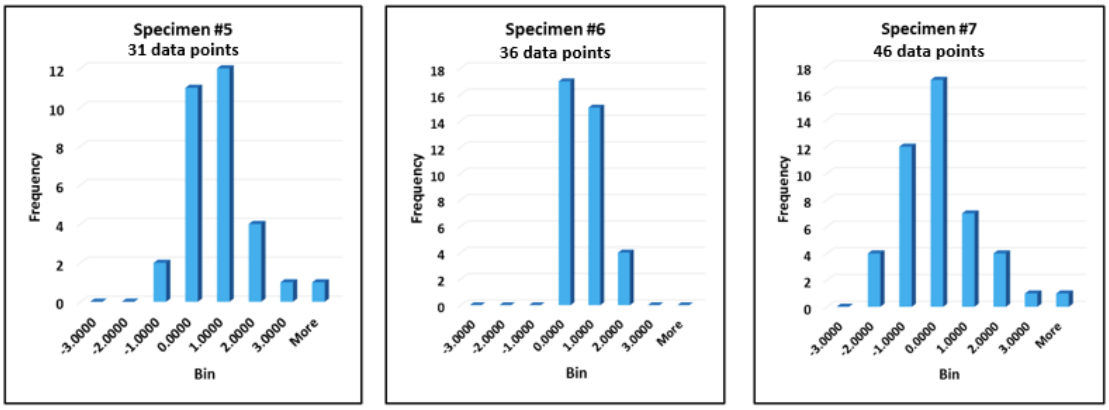

Figure 36: Frequency plot for specimen types 5, 6 and 7. Aluminum 24S-T3.

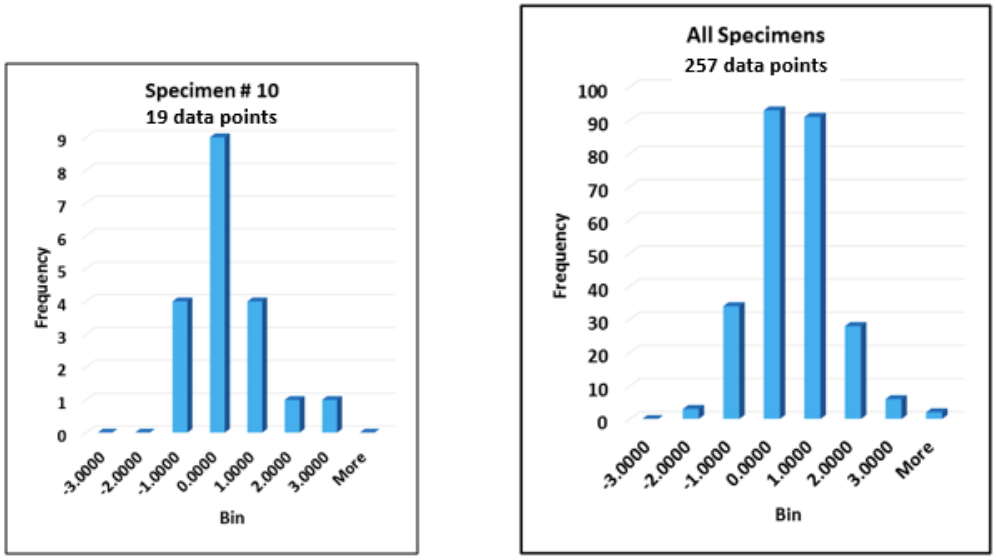

Figure 37: Frequency plot for specimen type 10 (left) and for all the specimens combined (right). Aluminum 24S-T3.

The combined frequency plots for all the specimen types of aluminum 75S-T6 (α = 1.0) and steel SAE-4130 (α = 0.0) are shown in Figure 38. The complete data set for each material is available in the Excel files: BetaZ-Score-Alpha-1.0(75S-T6).xlsx and BetaZ-Score-Alpha-0.0(SAE-4130).xlsx, respectively.

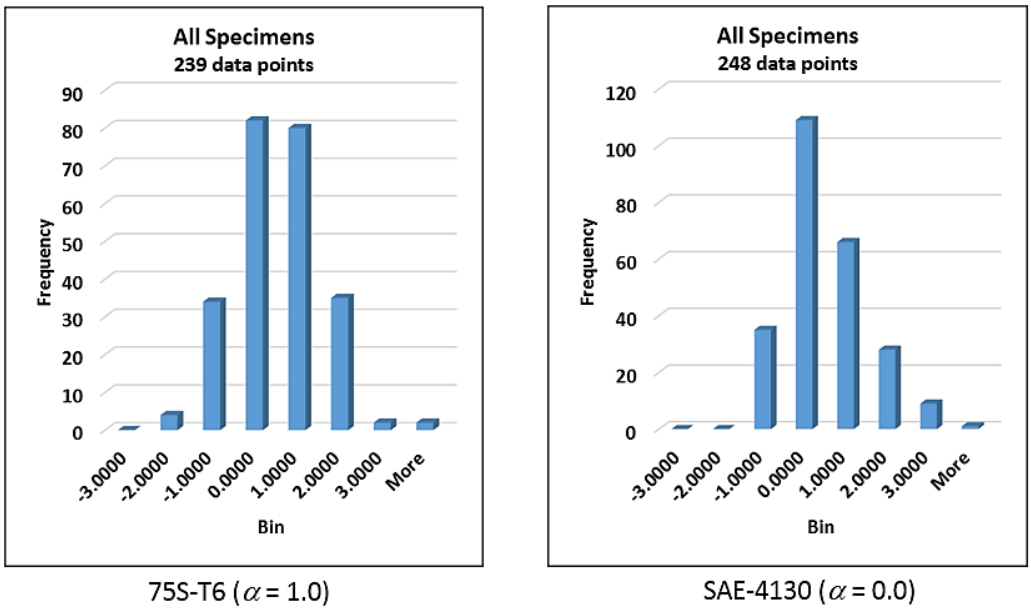

Figure 38: Frequency plots for all the specimens combined. Aluminum 75S-T6 and Steel SAE-4130.

Finally, a quantile of input sample v. quantile of lognormal distribution for all 9 specimen types of aluminum 24S-T3 for $\alpha = 0.8$ (a QQ plot) is shown in Figure 39.

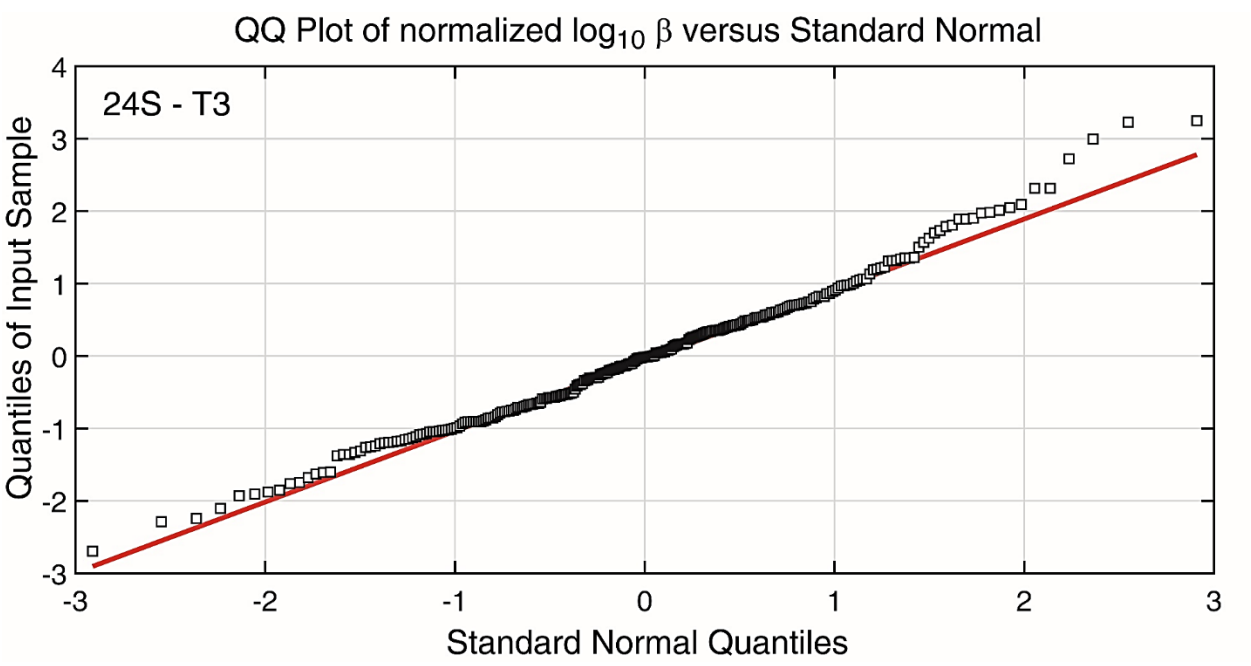

Figure 39: QQ plot for all 9 specimen types of aluminum 24S-T3 for $\alpha = 0.8$.

3 Summary and Conclusions

The focus of activities in the Option 3 Period of this contract was to expand the work initiated during the Option 1 & 2 periods [10, 11] for the support of flaw-tolerant design, certification and sustainment based on a reliable predictive capability for the estimation of the expected life of metallic airframe components, given part specifications, material properties, initial flaws and design load spectra.

During the Option 2 Period the focus was on providing a framework and recommendations for the development of stress-based damage accumulation models including the extension of the models for multiaxial loading. Stress-based damage accumulation models using the integral average of a function of stress over a solution-dependent volume characterized by a single parameter (β) provided a basis for ranking in-service damage from the point of view of fatigue criticality.

During the Option 2 Period we found that the best results were obtained when the highly stressed volume (*HSV*) of material around a flaw was correlated with β, allowing the generalization of the calibration work performed during Option 1 Period for flaw-seeded specimens of 7075-T73 Forging and Ti-6Al-4V beta STOA Forging to components with flaws of various sizes and shapes. It was also demonstrated that the effective stress computed using the notch sensitivity factor q as used by the classical methods to account for the effects of notches on the predicted fatigue life of structural components, is equivalent to computing the average stress over a solution-dependent domain defined by β. This approach allows the extension of the classical methods developed for notches to flaws of arbitrary shape.

During the Option 3 (Task 6) we described the step-by-step procedures to obtain the reference S-N curve from unnotched NACA specimens of 24S-T3, 75S-T6 and SAE 4130; the calibration procedures to obtain the β-*HSV* curves for each material utilizing the fatigue data from notched NACA specimens, and the prediction of fatigue life based on the calibration curve, including the measure of the difference between model prediction and the experimental results.

The SimGov Data Management Portal (https://ftd.esrd.com) was updated with the material developed during the Task 6, Option 3 Period, as shown in Appendix 4.

4 References

1. Szabó B, Actis R and Rusk D. “Predictors of fatigue damage accumulation in the neighborhood of small notches”. International Journal of Fatigue. Vol. 92, pp. 52-60, 2016.
2. Babuska I, Sawlan Z, Scavino M, Szabo B and Tempone R. “Bayesian inference and model comparison for metallic fatigue data”. Comput. Methods Appl. Mech. Engng. Vol. 304 pp. 171–196, 2016.
3. Pascual FG and Meeker WQ. “Analysis of fatigue data with runouts based on a model with nonconstant standard deviation and a fatigue limit parameter”. Journal of Testing and Evaluation. Vol. 25(3), pp. 292-301, 1997.
4. Pascual FG and Meeker WQ. “Estimating Fatigue Curves with the Random Fatigue-Limit Model”. Technometrics, vol. 41(4), pp. 277-290, 1999.
5. Smith KN, P. Watson, and T. H. Topper, “A Stress-Strain Function for the Fatigue of Metals”, Journal of Materials, ASTM, vol. 5, No. 4, pp. 767-778, 1970.
6. Szabó B, Actis R and Rusk D. “On the Formulation and Application of Design Rules”. Computers and Mathematics with Applications, 2017.
7. Pascual FG. “A Standardized Form of the Random Fatigue-Limit Model”. Communications in Statistics. Simulation and Computation. Vol. 32, No. 4, pp. 1205-1221, 2003.
8. Sines G. “Behavior of Metals under Complex Static and Alternating Stresses”. Chapter 7 in Sines G and Waisman JL (Editors) Metal Fatigue. McGraw Hill, New York 1959.
9. B. Szabó and R. Actis, "Simulation Governance: Technical Requirements for Mechanical Design," Comput. Methods Appl. Mech. Engrg, vol. N/A, no. In Press, p. N/A, 2012
10. Actis R, Szabó B, Watkins M and Hawks J. Innovative Approaches to Flaw-Tolerant Design and Certification of Airframe Components. Final Project Report for Option 1: Navy SBIR 2008.2 - Topic N08-131, Contract No. N68335-10-C-0428, 2014.
11. Actis R, Szabó B, Watkins M and Hawks J. Innovative Approaches to Flaw-Tolerant Design and Certification of Airframe Components. Final Project Report for Option 2: Navy SBIR 2008.2 - Topic N08-131, Contract No. N68335-10-C-0428, 2015.

Appendix 1: The statistical model $\mathcal{S}_2$

The statistical model $\mathcal{S}_2$ differs from the statistical model $\mathcal{S}_1$ only in that the standard deviation is assumed to be a function of σ_{eq}. We will use the functional form proposed by Pascual and Meeker in [3]:

$$s = 10^{B_1 + B_2 \log_{10} \sigma_{eq}} \qquad \textbf{A-1}$$

Therefore the statistical model $\mathcal{S}_2$ is characterized by six parameters $\theta_2 = \{A_1\ A_2\ B_1\ B_2\ \mu_f\ s_f\}$. The computed parameter values are shown in Figure 40.

Statistical Model S2 NACA materials: RFL, variable STD			
	24S-T3	75S-T6	SAE 4130
A1	7.344	6.279	7.177
A2	2.053	1.484	1.717
B1	-9.509	1.137	-6.083
B2	5.237	-1.242	2.946
mu_f	1.329	1.430	1.734
s_f	0.0619	0.0398	0.0397

Input and output parameters			
	24S-T3	75S-T6	SAE 4130
U	35	35	75
L	15	15	45
s_f	0.05	0.05	0.05
LL	-572.85	-879.89	-477.30
AIC	1155.7	1769.8	964.6

Parameters for the design curves			
	24S-T3	75S-T6	SAE 4130
A1	14.458	5.320	5.261
A2	6.423	0.972	0.814
A3	-0.367	21.200	40.387

Figure 40: Unnotched NACA data. Computed and input parameters for statistical model 2. Parameters for the design curve are for *p*=0.001.

The function called *MMPDSmodel2RFL(mat).m* is the main routine for Model $\mathcal{S}_2$. Its operation is analogous to that of Model $\mathcal{S}_1$. The PDF and the CDF functions are called *custpdfRFL2.m* and *custcdfRFL2.m* respectively.

For Model $\mathcal{S}_2$ the seed values B_1 and B_2 are estimated from

$$\log_{10} s = B_1 + B_2 \log_{10} \sigma_{eq}$$

Letting

$$s_j = \left| \log_{10} N_j - \left(A_1^{(I)} - A_2^{(I)} \log_{10} (\sigma_{eq} - A_3^{(I)}) \right) \right|$$

And $x_j = \log_{10} \sigma_{eq}^{(j)}$, $y_j = \log_{10} s_j$ we find B_1, B_2 by linear regression using

$$y_j \approx B_1 + B_2 x_j, \quad j = 1, 2, \ldots, n_I$$

The computations are performed using the Matlab function *SeedValuesS2.m*. The seed values for Model $\mathcal{S}_2$ are:

$$\theta_{seed}^{(2)} = \left\{ A_1^{(I)}\ A_2^{(I)}\ B_1\ B_2 \log_{10}\left(A_3^{(I)}\right)\ 0.05 \right\}$$

Discussion

Since Model $\mathcal{S}_1$ is a special case of Model $\mathcal{S}_2$, we must have $LL(\hat{\theta}_1) < LL(\hat{\theta}_2)$. This is found to hold numerically for the three materials investigated. The AIC values take into consideration the number of parameters used in the statistical model. The AIC values are consistently smaller for $\mathcal{S}_1$ than for $\mathcal{S}_2$, therefore $\mathcal{S}_2$ is more efficient than $\mathcal{S}_1$.

Anomalous behavior is exhibited by $\mathcal{S}_2$ for the 24S-T3 and SAE 4130 materials, however. One expects the standard deviation to increase with decreasing σ_{eq} values therefore the parameter B_2 in Eq. (A-1) should be negative. On the contrary, we find that for these two materials B_2 is positive and B_1 is negative (see Figure 40).

It was possible to find parameters $\hat{\theta}_2$ such that B_2 was negative through experimenting with various seed parameter values, however in those cases $LL(\hat{\theta}_1) > LL(\hat{\theta}_2)$ which clearly indicates that those parameters do not correspond to a local minimum. It is also surprising that the parameter A_3 of the design curve is negative for 24S-T3. The design curve shown in Figure 41 for Model $\mathcal{S}_2$ is comparable with the design curve shown in Figure 1 for Model $\mathcal{S}_1$.

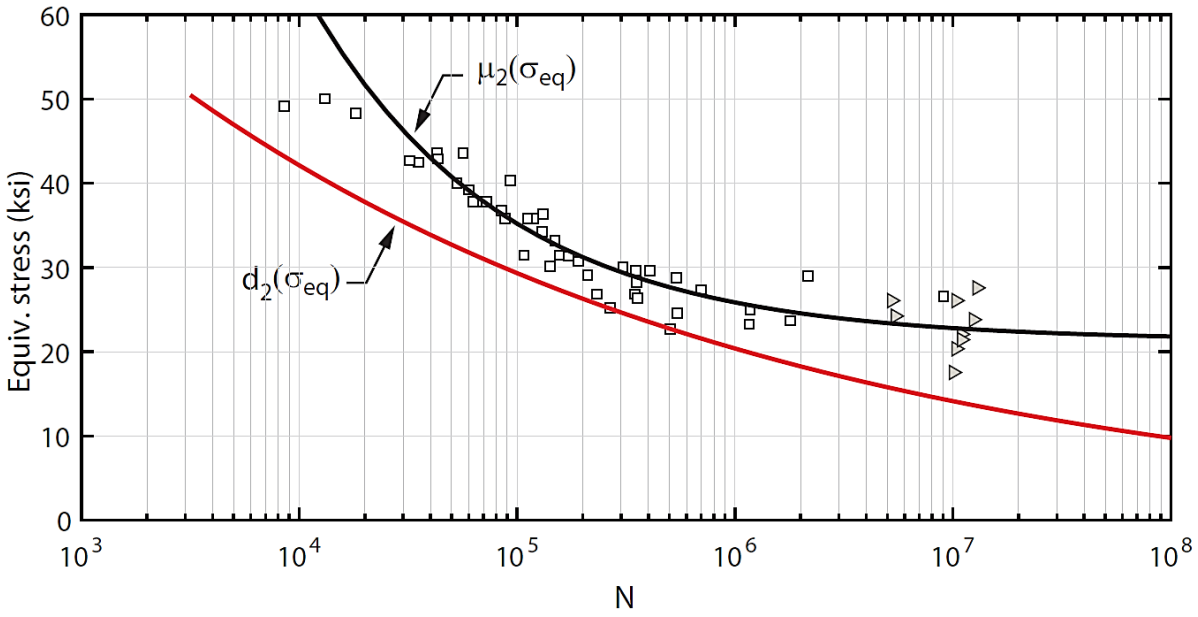

Figure 41: S-N data for 24S-T3 aluminum alloy. The mean corresponding to Model $\mathcal{S}_2$ is labeled $\mu_2(\sigma_{eq})$, the theoretical design curve corresponding to $p = 0.001$ is labeled $d_2(\sigma_{eq})$. Runouts are represented by the triangular markers.

Appendix 2: Comments on the Random Fatigue Limit Model

On page 279 in reference [4] the marginal cumulative distribution for the normal-normal model is defined as follows:

$$F(w;x,\boldsymbol{\theta}) = \int_{-\infty}^{x} \frac{1}{\sigma_\gamma} \Phi_{W|V}\left(\frac{w-\mu(x,v,\boldsymbol{\theta})}{\sigma}\right) \phi_V\left(\frac{v-\mu_\gamma}{\sigma_\gamma}\right) dv \qquad \text{A-2}$$

Where

$$\Phi_{W|V}\left(\frac{w-\mu(x,v,\boldsymbol{\theta})}{\sigma}\right) = \frac{1}{2}\left(1+\operatorname{erf}\left(\frac{w-(\beta_0+\beta_1\log[\exp(x)-\exp(v)]}{\sigma\sqrt{2}}\right)\right) \qquad \text{A-3}$$

and

$$\phi_V\left(\frac{v-\mu_\gamma}{\sigma_\gamma}\right) = \frac{1}{\sqrt{2\pi}}\exp\left(-\frac{(v-\mu_\gamma)^2}{2\sigma_\gamma^2}\right) \qquad \text{A-4}$$

Let us consider the normal-normal model. From Table 1 in [4] we get:

$$\beta_0 = 30.272, \quad \beta_1 = -5.1000, \quad \sigma = 0.289, \quad \mu_\gamma = 5.366, \quad \sigma_\gamma = 0.031$$

Using these data we compute the marginal CDF for various stress levels. The results are shown in Figure 42. In the neighborhood of $s = \exp(\mu_\gamma) \approx 214$ MPa, the CDF values do not appear to converge to 1 as $w \to \infty$. The reason for this is that for large w the function $\Phi_{W|V}$ is unity independent of x (where, by definition, $x = \log s$). On the other hand, the integral of ϕ_V depends on x. Therefore for $w \to \infty$ we have

$$F(w;x,\boldsymbol{\theta}) \to g(x,\boldsymbol{\theta}) := \int_{-\infty}^{x} \frac{1}{\sigma_\gamma\sqrt{2\pi}}\exp\left(-\frac{(v-\mu_\gamma)^2}{2\sigma_\gamma^2}\right) dv. \qquad \text{A-5}$$

The computed values of $g(x, \theta)$ are shown in Table 1 and displayed in Figure 42. It is seen that $g(x, \theta)$ is sensitive to s when x is close to μ_γ.

In conclusion, the marginal CDF and PDF functions should be scaled by $1/g(x, \theta)$ to ensure that the CDF is unity for large w, independent of s. This scaling affects the definition of the likelihood function and hence $\boldsymbol{\theta}$.

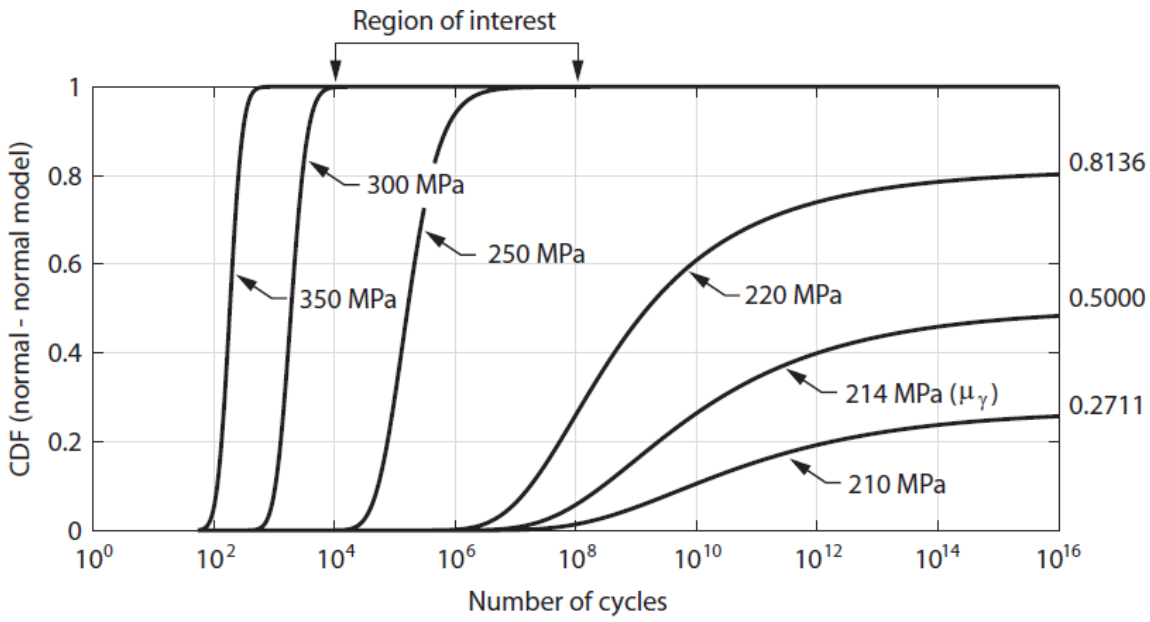

Figure 42: Cumulative distribution functions corresponding to the indicated stress levels.

Table 12: The computed values of $g(x, \theta)$ corresponding to the stress values shown in Figure 42. The stress values are in MPa units.

	$s = 350$	$s = 300$	$s = 250$	$s = 220$	$s = 214$	$s = 210$
$g(x, \boldsymbol{\theta})$	1.0000	1.0000	1.0000	0.8136	0.5000	0.2711

Correspondence on this point with Professors Pascual and Meeker is reproduced in the following.

Correspondence with Professors F. G. Pascual and W. Q. Meeker

Date: Sat, 12 Nov 2016 13:15:23 +0000
From: "Szabo, Barna" <szabo@wustl.edu>
To: "wqmeeker@iastate.edu" <wqmeeker@iastate.edu>,
"jpascual@math.wsu.edu" <jpascual@math.wsu.edu>
Subject: Question relating to the random fatigue limit model

Dear Professors Pascual and Meeker,

With reference to your joint paper published in Technometrics in 1999, I believe that the marginal PDF and CDF functions defined in that paper should be scaled as explained in the appended note.

I will greatly appreciate if you would let me know whether you agree with the conclusion.

With best regards,

Barna Szabo

From: Jave Pascual <jpascual@math.wsu.edu>
Sent: Monday, November 14, 2016 1:10 PM
To: Szabo, Barna
Cc: Jave Pascual; wqmeeker@iastate.edu
Subject: Re: Question relating to the random fatigue limit model

Professor Szabo,

Thanks for interest in the RFL model. Below are some thoughts related to your inquiry:

One of the motivations for the RFL model was to "model" infinite life whenever the unit's fatigue limit exceeded applied stress. One way of looking at it is that there is a positive probability mass at infinite life and that probability is the same as the probability that a unit's fatigue limit falls above the applied stress. Infinite life and the "probability deficit" are still accounted for in the likelihood when we compute survival= 1-cdf.

Also, when you normalize or standardize the pdf or cdf, you convert marginal to conditional probabilities wherein you are making the additional assumption that the fatigue limit is lower than the applied stress FOR ALL units.

The feature of placing a distribution on the fatigue limit allows the model to mechanistically (as opposed to curve-fitting) describe the curvature that we often see in the S/N curve.

Jave

F. G. Pascual

Associate Professor
Department of Mathematics and Statistics
Washington State University
PHONE: (509)335-3126
FAX: (509)335-8369
E-MAIL: jave@wsu.edu

Meeker, William Q [STAT] <wqmeeker@iastate.edu>

Dear Professor Szabo:

The distribution, as written in the paper is correct. A feature of the RFL model is that there is always a positive probability that life will extend to infinity. Think of it this way. The fatigue limit is a random variable, but once it is realized on a given unit, it is fixed. If the applied constant stress for that unit is less than the fatigue limit, then a crack will never initiate.

Best regards,

Bill Meeker

Remarks

If the conditional PDF is not scaled then, as seen in Figure 42, when the applied stress is equal to μ_γ (214 MPa) then there is a 50% chance for infinite life. This does not seem plausible.

Scaling the conditional PDF means that failure will always occur. Using the scaled PDF should be considered as an alternative to the RFL model proposed by Pascual and Meeker in [4]. Pascual proposed yet another variant of the RFL model in [7].

As noted by Professor Pascual, scaling converts marginal probability to conditional probability implying the assumption that the fatigue limit may be zero. As a practical matter this is not a concern because the calibration data would not justify extrapolation beyond 100 million cycles.

We should note also that aluminum alloys, unlike ferrous and titanium alloys, do not have a fatigue limit. Therefore the fatigue limit model, applied to these materials, should not be considered valid for fatigue cycles exceeding some limit which is not greater than 10^8.

Appendix 3: Configuration of the specimens identified in Table 2

NACA specimen dimensions and corresponding finite element meshes used for the analysis.

- Specimen # 1 – Unnotched dogbone specimen – Actual K_t = 1.00

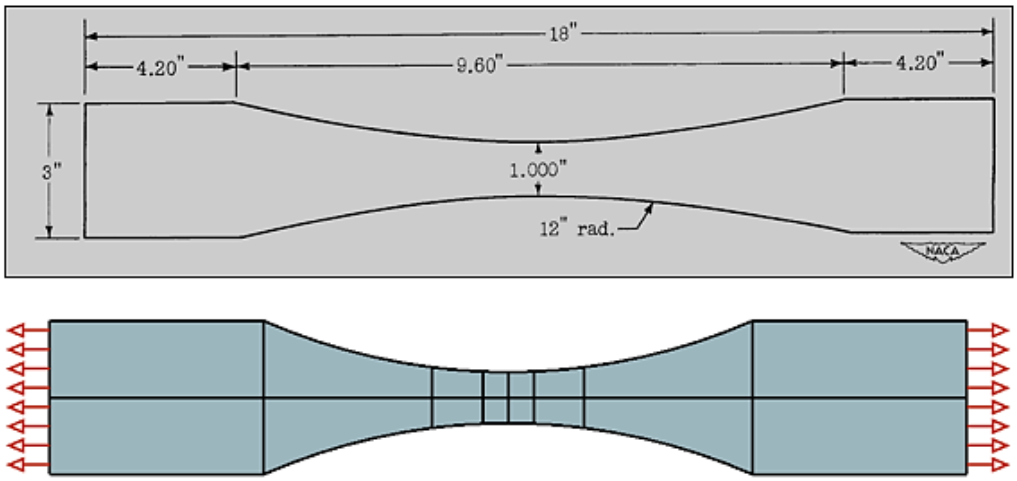

- Specimen #2 – Hole type notch – Actual K_t = 2.11

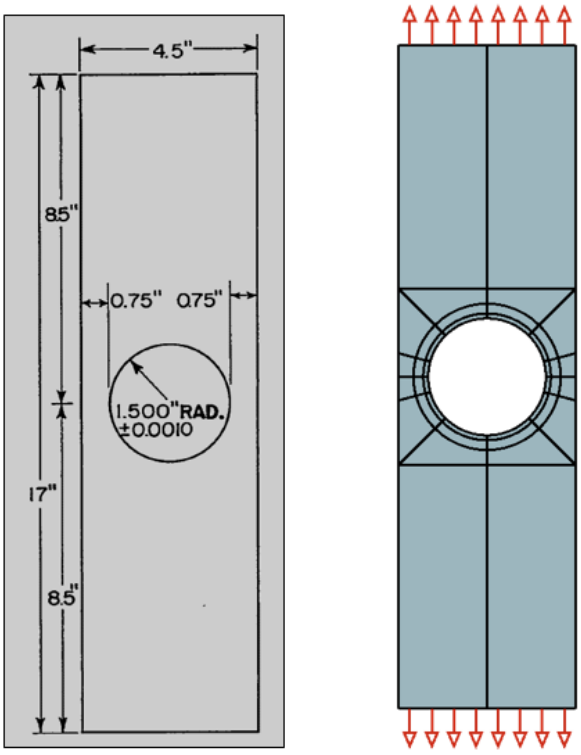

- Specimen #3 – Edge-cut notch – Actual K_t = 2.17

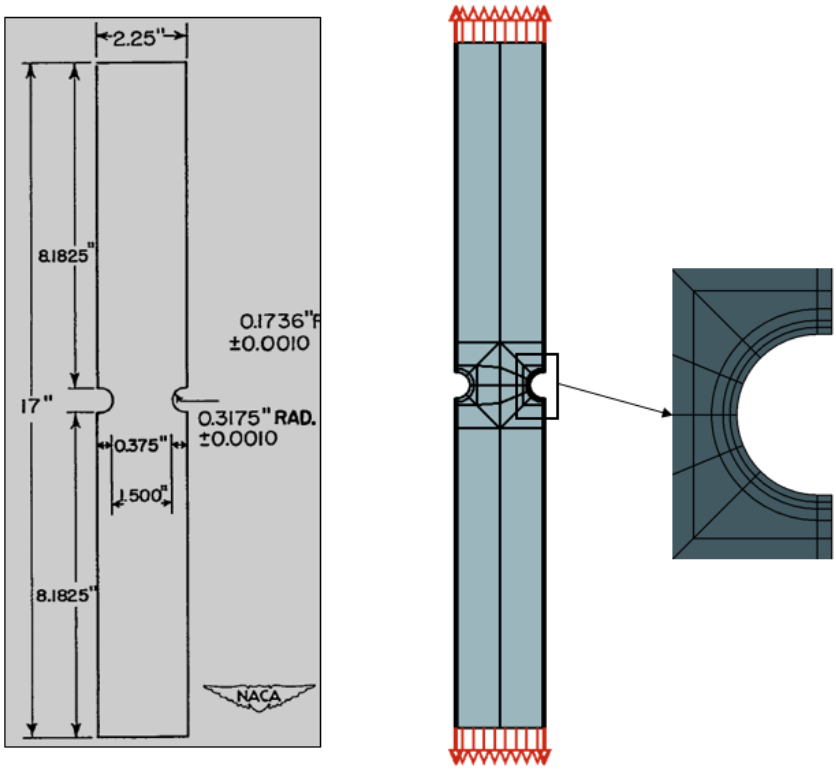

- Specimen #4 – Fillet-type notch – Actual K_t = 2.19

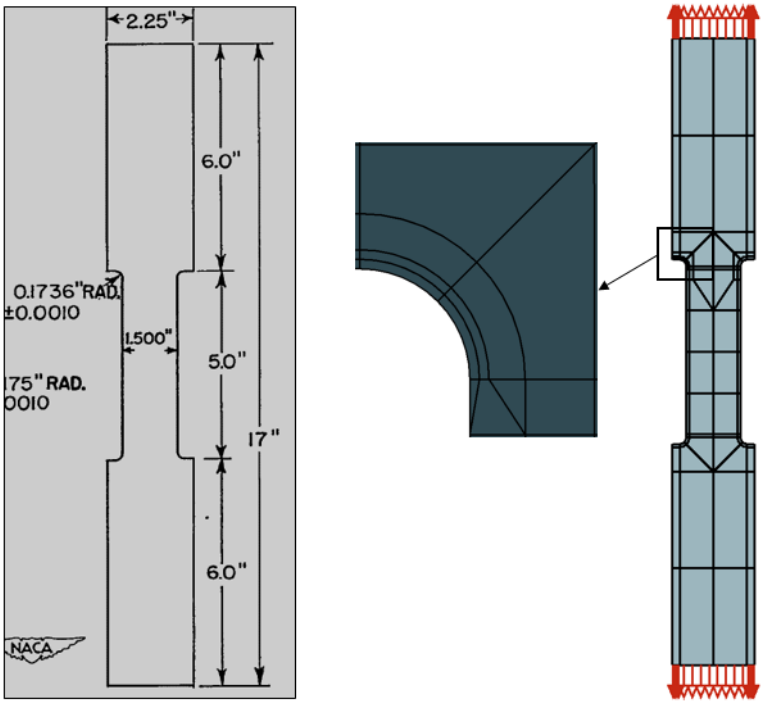

- Specimen #5 – Edge-cut notch – Actual K_t = 4.43

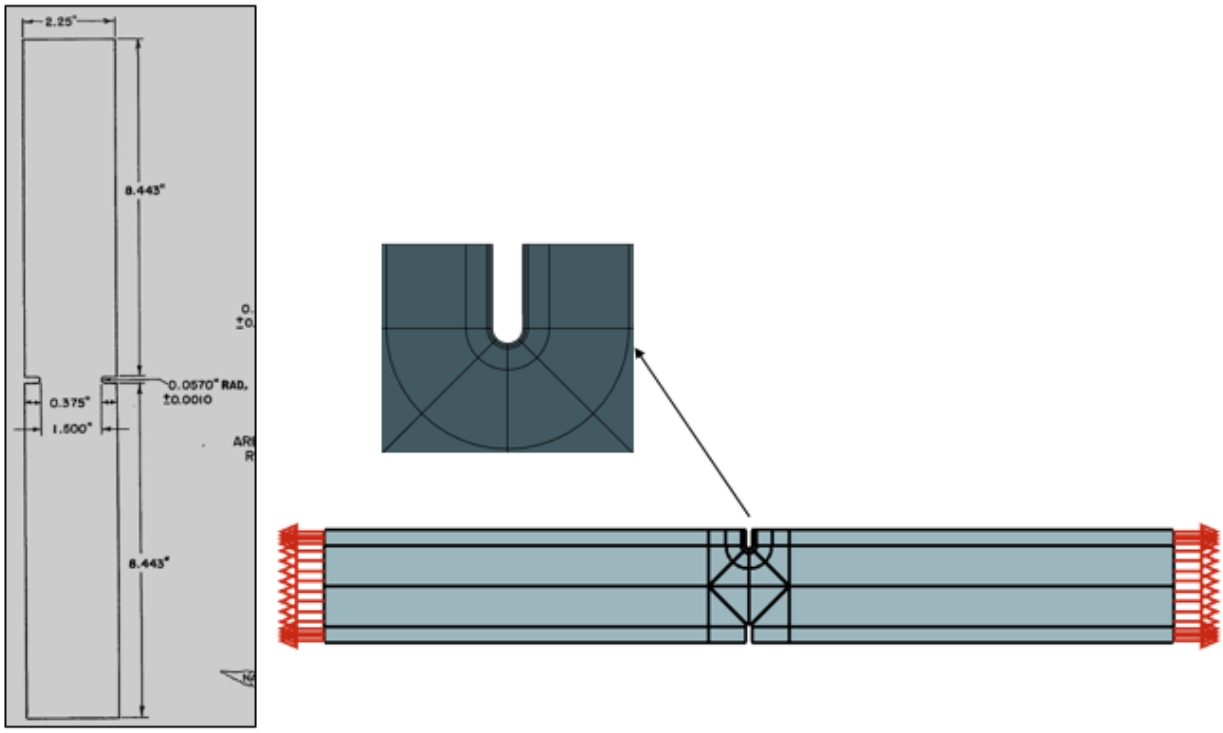

- Specimen #6 – Fillet-type notch – Actual K_t = 4.83

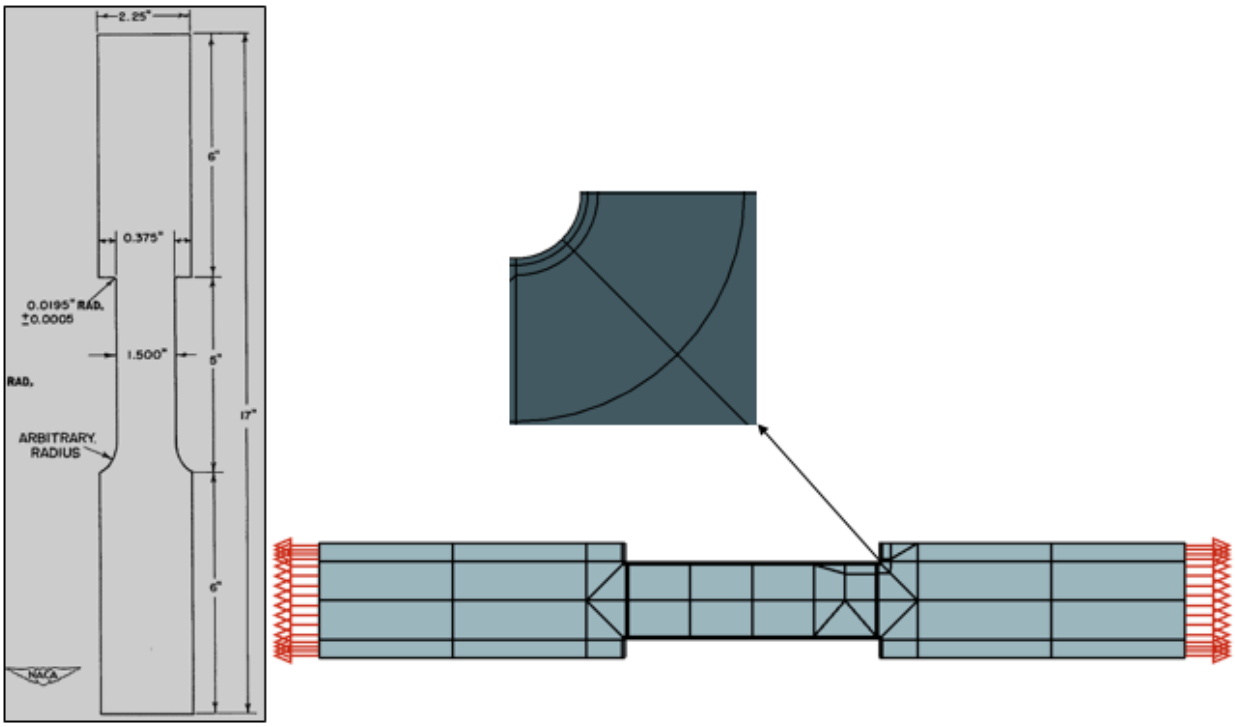

- Specimen #7 – Edge-cut notch – Actual K_t = 5.83

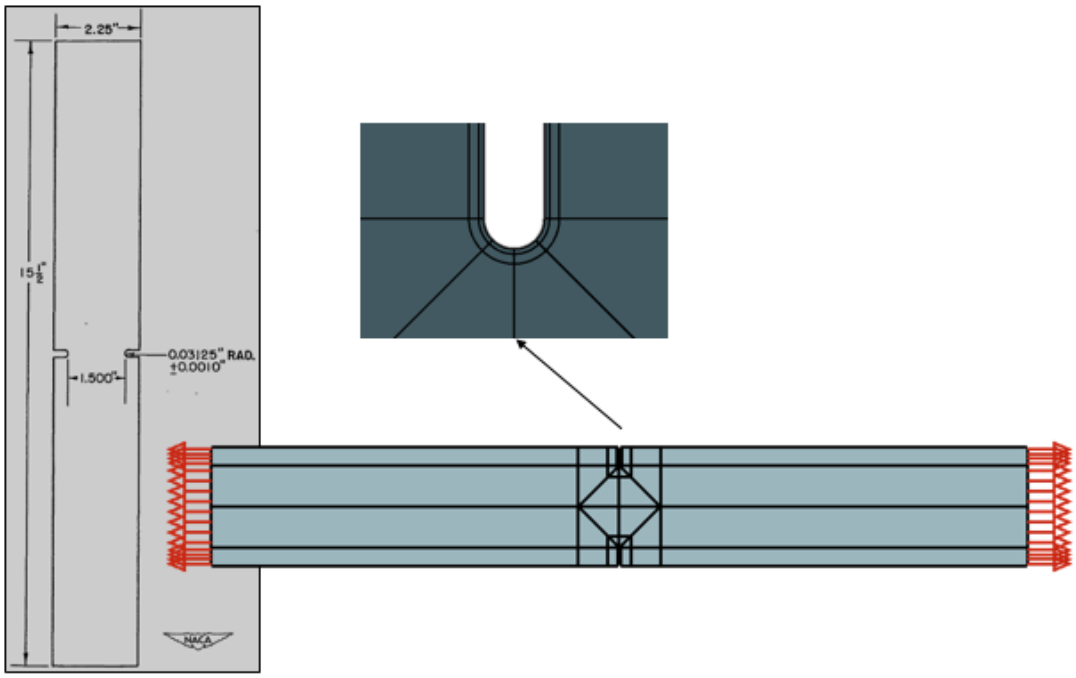

- Specimen #8 – Edge-cut notch – Actual K_t = 1.62

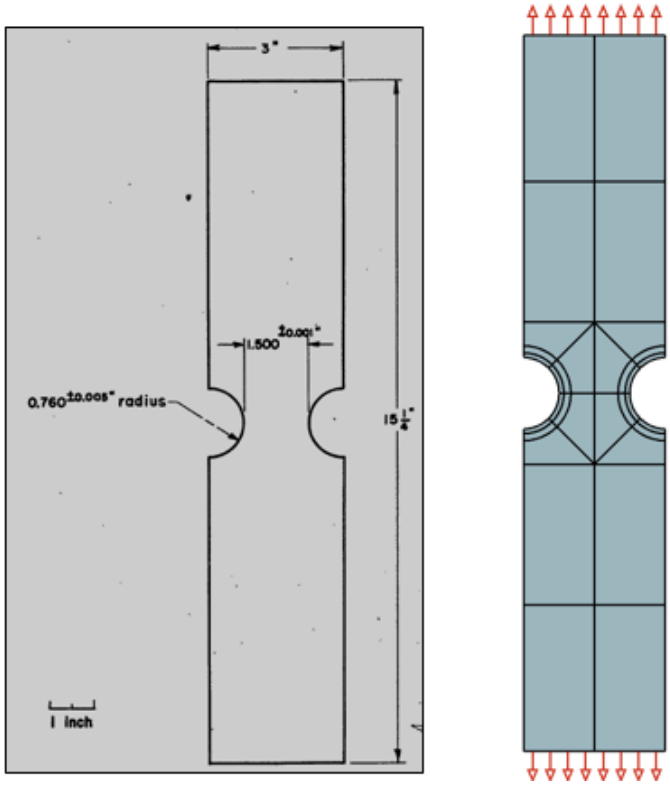

- Specimen #9 – Edge-cut notch – Actual K_t = 4.48

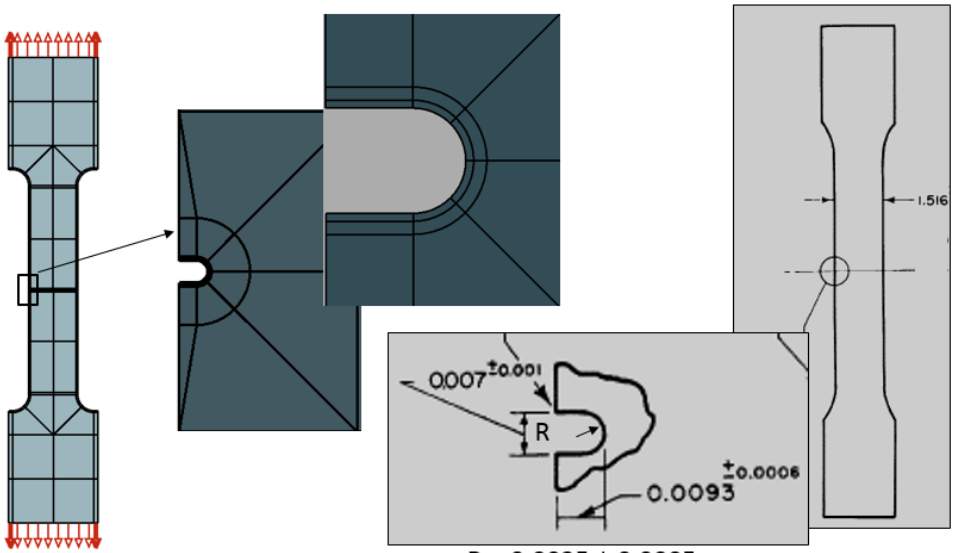

- Specimen #10 – Edge-cut notch – Actual K_t = 4.41

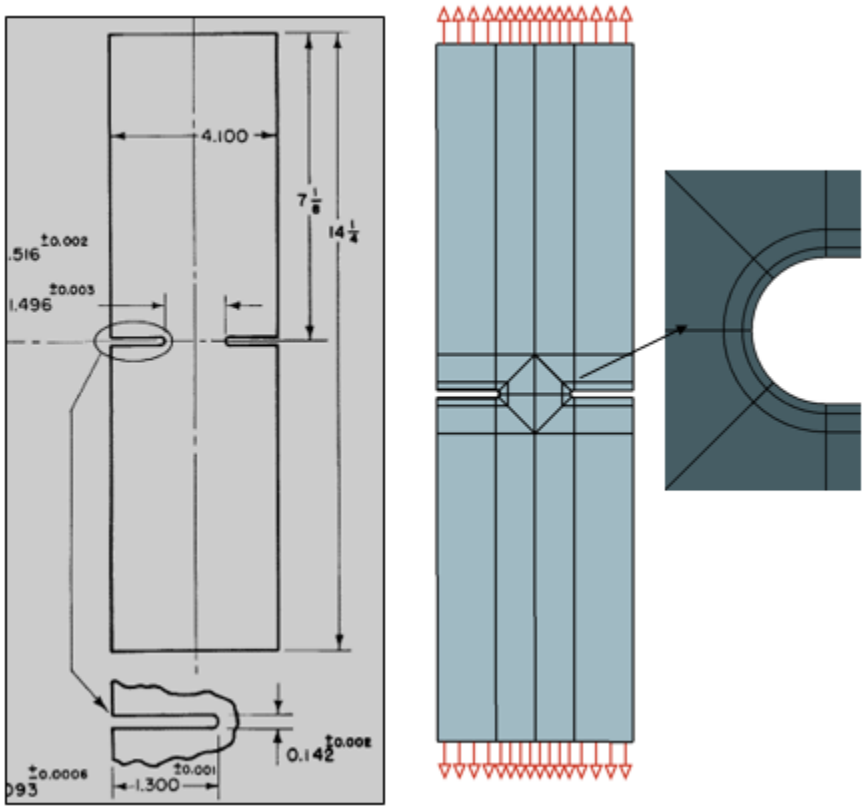

Appendix 4: Updates to SimGov Portal during the Task 6 of the Option 3 Period

All files for Task 6 referenced throughout this report are located in the *SimGov Data Management Portal* https://ftd.esrd.com, under the Data Group **NACA Data**. The file names and contents are as follows:

1. Model S1 Archived.zip and Model S2 Archived.zip – Matlab functions and input data for statistical models $\mathcal{S}_1$, and $\mathcal{S}_2$, according to the details given in Section 2.3 and in Appendix 1.
2. naca-tn-24S-T3-(Raw Data).xlsx – Fatigue data of 93 unnotched specimen extracted from NACA-TN-2324, Table 2 is tabulated in this Excel file, worksheet "Kt=1 data". Of the 93 specimens, 10 were runouts and 11 were disqualified tests.
3. naca-tn-75S-T6-(Raw Data).xlsx – Fatigue data of 86 unnotched specimen extracted from NACA-TN-2324, Table 3 is tabulated in this Excel file, worksheet "Kt=1 data". Of the 86 specimens, 12 were runouts and 3 were disqualified tests.
4. naca-tn-SAE-4130-(Raw Data).xlsx – Fatigue data of 59 unnotched specimen extracted from NACA-TN-2324, Table 4 is tabulated in the Excel file, worksheet "Kt=1 data". Of the 59 specimens, 16 were runouts and 6 were disqualified tests.
5. BetaSummary24S-T3.xlsx – Values of the parameter β computed for all test cases of the eight specimen types used for calibration, and for values of a = 0.0, 0.2, 0.4. 0.5, 0.6, 0.8, 1.0. Material aluminum 24S-T3.
6. BetaSummary75S-T6.xlsx – Values of the parameter β computed for all test cases of the eight specimen types used for calibration, and for values of a = 0.0, 0.2, 0.4, 0.5, 0.6, 0.8, 1.0. Material aluminum 75S-T6.
7. BetaSummarySAE-4130.xlsx – Values of the parameter β computed for all test cases of the eight specimen types used for calibration, and for values of a = 0.0, 0.2, 0.4, 0.5, 0.6, 0.8, 1.0. Material steel SAE-4130.
8. FittedBetaSummary.xlsx – Summary of β-values computed from Eq. (30) and Eq. (31) for specimen 9, all materials (see Table 3); summary of Bayes factors for specimen 9, all materials (see Table 4); summary of optimal values of α for each material and β-fit (see Table 11). Macro Excel files used for the computations of the β values for each test case of the 8 specimens types used for calibration are in the following files (with *xx* = 00, 02, 04, 05, 06, 08, 10):
    - Prediction (24S-T3 SWT)-RFL-Model-1-Alpha-*xx*.xlsm
    - Prediction (75S-T6 SWT)-RFL-Model-1-Alpha-*xx*.xlsm
    - Prediction-SAE-4130-RFL-Model-1-Alpha-*xx*.xlsm

9. RankingData-24S-T3-Specimen-9.xlsx – Ranking of β prediction using Eq. (26) to compute $G_{\alpha_j}^{(i)}$, given $\bar{\beta}(\alpha_j, HSA)$ and $\beta_{AVG}(\alpha_j, HSA)$, for each of the test records corresponding to specimen #9. Material aluminum 24S-T3.
10. RankingData-75S-T6-Specimen-9.xlsx – Ranking of β prediction using Eq. (26) to compute $G_{\alpha_j}^{(i)}$, given $\bar{\beta}(\alpha_j, HSA)$ and $\beta_{AVG}(\alpha_j, HSA)$, for each of the test records corresponding to specimen #9. Material aluminum 75S-T6.
11. RankingData-SAE-4130-Specimen-9.xlsx – Ranking of β prediction using Eq. (26) to compute $G_{\alpha_j}^{(i)}$, given $\bar{\beta}(\alpha_j, HSA)$ and $\beta_{AVG}(\alpha_j, HSA)$, for each of the test records corresponding to specimen #9. Material steel SAE-4130.
12. Calibration-All-(24S-T3-SWT)-RFL-Model-1-Alpha-02.xlsm and Calibration-All-(24S-T3-SWT)-RFL-Model-1-Alpha-08.xlsm – Updated *β-HSA* calibration curves for all nine specimen types for the optimal values of α. Material aluminum 24S-T3.
13. Calibration-All-(75S-T6-SWT)-RFL-Model-1-Alpha-06.xlsm and Calibration-All-(75S-T6-SWT)-RFL-Model-1-Alpha-10.xlsm – Updated *β-HSA* calibration curves for all nine specimen types for the optimal values of α. Material aluminum 75S-T6.
14. Calibration-All-SAE-4130-RFL-Model-1-Alpha-00.xlsm – Updated *β-HSA* calibration curves for all nine specimen types for the optimal value of α. Material steel SAE-4130.
15. BetaZ-Score-Alpha-0.8(24S-T3).xlsx – Detailed computation of the frequency plots described in Section 2.5.1. Material aluminum 24S-T3 for $\alpha = 0.8$.
16. BetaZ-Score-Alpha-1.0(75S-T6).xlsx – Detailed computation of the frequency plots described in Section 2.5.1. Material aluminum754S-T6 for $\alpha = 1.0$.
17. BetaZ-Score-Alpha-0.0(SAE-4130).xlsx – Detailed computation of the frequency plots described in Section 2.5.1. Material steel SAE-4130 for $\alpha = 0.0$.